Chapter 4
Adsorption of Chromium from aqueous solutions using Polyaniline

4.1 Introduction

The use of conductive polymers for the removal of Cr^{6+} has gained more interest due to their reversibility and high efficiency. Polyaniline (PANI) is one of the most extensively investigated conducting polymers because of its good stability, low cost, environment friendliness and can be synthesized at large scale at low cost (Bhadra, Khastgir, Singha, & Lee, 2009). It is well-known that polyaniline exists in three different oxidation states, polyemeraldine (EB), leucoemeraldine (LB) and pernigraniline (PB) of which only polyemeraldine (EB) is electrically conductive (Ogoshi et al., 2011).

The use of PANI for the reduction of more toxic Cr^{6+} to less toxic Cr^{3+} has been reported (Ruotolo & Gubulin, 2005. The Cr^{6+} can be effectively reduced to Cr^{3+} because of its good reduction behaviors with the electron transfer from the LB or EB states to PB state.

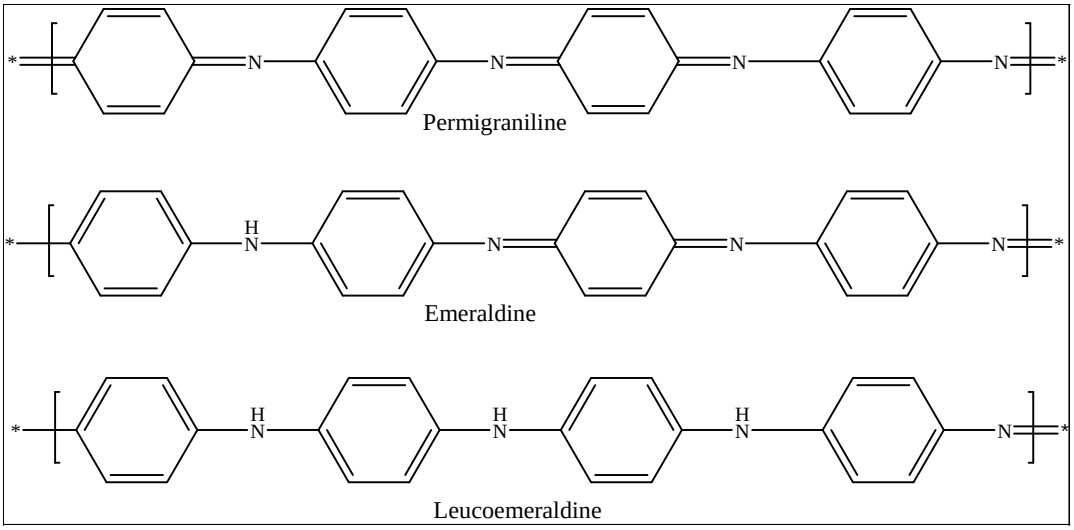

Figure 4.1 Different form of PANI

The spontaneous reduction of Cr^{6+} ions to Cr^{3+} ions is also possible by surface chemical reaction with PANI (Krishnani et al., 2013;). Breslin and co-worker (Farrell & Breslin, 2004) have studied the mechanism and kinetics of Cr^{6+} reduction by various oxidation states of electrochemically synthesized polyaniline films. They have also reported the effect of polyaniline film thickness on the efficiency of reduction process. Cr^{6+} removal has also been tested by electro synthesized PANI films (Jianqiang Wang, Pan, He, & Cao, 2013). Olad et al have used chemically and electrochemically synthesized polyaniline in powder and film forms

for the reduction of Cr^{6+} to Cr^{3+} in aqueous solutions. They observed that the reductive performance of the polymer for Cr^{6+} is increased with increasing thickness of the polyaniline films prepared electrochemically in contrast to chemically synthesized polymer films,. Further, they also observed that high concentrations of Cr^{6+} resulted in over oxidation and degradation of all forms of polyaniline and in acidic conditions degradation of polyaniline occurs even in lower concentrations of Cr^{6+}.However, increasing the acidity of Cr^{6+} solutions increased the kinetics and efficiency of reduction (Olad & Nabavi, 2007).. PANI powders with rough surface are amenable for highly efficient Cr^{6+} removal due to their large specific surface area, low cost and easy bulk production (Chiou & Epstein, 2005; Guo, Fei, Su, & Zhang, 2011; Huang & Kaner, 2006).

The efficiency and kinetics of Cr^{6+} removal by various forms of PANI film and powder, have also been compared (Jianqiang Wang et al., 2013). By contrast with the powder form, PANI films were found to be difficult to fabricate and the penetration of the Cr^{6+} into the film interior was found to be limited. However, most of the previous studies have focussed on PANI films, which always have specific surface areas, typically up to 80 m^2/g (Germain, Fréchet, & Svec, 2007), and limited functional groups on the edge areas (Feng et al., 2011; Guo et al., 2011).

The commonly and widely used oxidant for PANI in the chemical polymerization method is ammonium persulfate (APS) (Gu, Guo, et al., 2013; G. Li, Li, Li, Peng, & Chen, 2011). The oxidants such as ferric chloride ($FeCl_3$) (Pan et al., 2006), Hydrogen peroxide (H_2O_2) (Jin, Su, & Duan, 2001), Perchloric acid ($HClO_4$) (K. Wang, Huang, & Wei, 2010), Vanadic acid (G. Li, Jiang, & Peng, 2007), Manganese dioxide (MnO_2) (Fei et al., 2009; Pan et al., 2007), Tetrachloroaurate $AuCl_4^-$ (X. Zhang, Chechik, Smith, Walton, & Duhme-Klair, 2008) and Cr^{6+} have also been reported to prepare PANI (Gu, Tadakamalla, et al., 2013). Gu et al observed that Cr^{6+} dose as oxidant influenced the PANI nanostructures as well as the crystallization structure (Gu, Wei, et al., 2013).

PANI showed significant changes in the electronic transport properties when doped with various anions via chemical routes (MacDiarmid et al., 1991). Traditionally, PANI is prepared in strong protonic acids like HCl and H_2SO_4, with aggregated granules as the main product. Recently, PANI is also prepared in other protonic acids or neutral water to modulate its morphology, processability and conductivity (Chakraborty, Mukherjee, & Mandal, 2000; Z. Zhang, Wei, & Wan, 2002). For example, Cao et al. (Cao, Smith, & Heeger, 1992) reported for the first time that functional protonic acids such as dodecylbenzenesulfonic acid increased the solubility of PANI in common organic solvents. Zhang et al. (Z. Zhang et al., 2002) reported that morphology

and electrical properties of PANI nanostructures depended on both dopant structures and reaction conditions. Trchova et al. (Trchova, Sedenkova, Konyushenko, Stejskal, & Ciric-Marjanovic, 2006) and Stejskal et al. (Jaroslav Stejskal, Sapurina, & Trchova, 2010) reported that depending on the acidity of the reaction solution, different PANI structures including granules, nanofibers and nanotubes could be obtained. PANI was prepared by a facile sono-assisted method in various protonic acids by wang et al. (Jing Wang, Zhang, & Zhao, 2014).

Runhu Zhang et al have used polyaniline doped with sulfuric acid for removal of Cr^{6+} from aqueous solution. The maximum uptake of Cr^{6+} was 95.79 mg g^{-1}(R. Zhang, Ma, & Wang, 2010). However they did not study whether Cr^{6+} was getting reduced to Cr^{3+}.

There have been various reports on the use of modified PANI and PANI composites for enhancing the removal of chromium(P. A. Kumar, Chakraborty, & Ray, 2008; Olad & Nabavi, 2007; Samani, Borghei, Olad, & Chaichi, 2010).

Ansari reported adsorption of Cr^{6+} from aqueous solutions using sawdust coated by PANI, PANI composites with nylon 66 and polyurethane (Ansari, 2006). Karthik et al. reported removal of hexavalent chromium ions using PANI/silica gel composite (Karthik & Meenakshi, 2014b). Polyacrylonitrile/PANI core/shell nanofiber mat was synthesized for removal of hexavalent chromium from aqueous solution (Jianqiang Wang et al., 2013).

PANI functionalized graphene sheets were used for effective removal of Cr^{6+} from water (Harijan & Chandra, 2016). The adsorption efficiency, acidic resistance, selectivity toward Cr^{6+} and mechanical strength of chitosan were improved by including amine-containing PANI type polymer chains, PAA and MWNTs, respectively, as well through the formation of IPN structure between them by Kim et al (Kim, Shanmuga Sundaram, Anantha Iyengar, & Lee, 2015). PANI coated magnetic Fe_3O_4, carbon fiber fabric and cellulose has been studied by Qiu et al. (Qiu et al., 2015) for Cr^{6+} removal.

PANI grafted magnetic mesoporous silica composite was successfully prepared by Tang et al. for Cr^{6+} removal from aqueous solution (Tang et al., 2014).Karthik et al. studied the removal of Cr^{6+} ions from aqueous solution using PANI/SiO_2 composite (Karthik & Meenakshi, 2014b).

Polypyrrole-polyaniline (PPy-PANI) nanofibers as adsorbent of Cr^{6+} was investigated by Bhaumik et al. (Bhaumik, Maity, Srinivasu, & Onyango, 2012). The adsorption of chromium compounds from solutions by a composite of polyaniline/poly ethylene glycol (PANI/PEG) was investigated by Samani et al. (Samani et al., 2010). PANI/humic acid composites have also been studied for the removal of chromium (Q. Li, Sun, Zhang, Qian, & Zhai, 2011).

PANI was synthesized on the surface of jute fiber and was used as an adsorbent to remove hexavalent chromium from wastewater by Kumar et al. (P. A. Kumar et al., 2008). Sodium alginate-polyaniline (SAP) nanofibers were evaluated as adsorbents for the removal of Cr^{6+} by Karthik et al. (Karthik & Meenakshi, 2015a). Chávez-Guajardo et al. investigated the use of PPY/c-Fe_2O_3 and PANI/c-Fe_2O_3 MNCs for removing Cr^{6+} and Cu^{2+} (Chávez-Guajardo et al., 2015). Kumar and Chakraborty developed a polyaniline/jute fiber composite adsorbent for Cr^{6+} removal (P. A. Kumar & Chakraborty, 2009). Kapok fiber (KF) was combined with PANI by Zheng et al. to obtain an adsorbent for removal of Cr^{6+} (Zheng, Wang, Huang, & Wang, 2012). Yavuz et al. synthesized alkyl-substituted polyaniline/chitosan (sPANIs/Ch-HCl) composites and applied it for the removal of Cr^{6+} from aqueous solutions (Yavuz, Dincturk-Atalay, Uygun, Gode, & Aslan, 2011).

Researchers have shown considerable attention towards synthesis of bio/conducting polymeric composites as adsorbents for the removal of Cr^{6+} ions from aqueous solution (Hena, 2010; Karthik & Meenakshi, 2014a, 2014b; Lei, Qian, Shen, & An, 2012; Liu, Zhou, Qian, Shen, & An, 2013; Yavuz et al., 2011). The adsorption performance of the DBSA doped Polyaniline/ MWCNTs hybrid for the removal of Cr^{6+} from aqueous solution was evaluated by kumar et al. (R. Kumar, Ansari, & Barakat, 2013). Karthik et al. coated chitin with polyaniline by in-situ polymerization method and employed as an adsorbent for the removal of Cr^{6+} ions (Karthik & Meenakshi, 2015b). The removal of Cr^{6+} ions from aqueous solution using cross linked chitosan-grafted-polyaniline composite (CCGP) was compared with that of chitosan-grafted-polyaniline (CGP) composite by Karthik et al. (Karthik & Meenakshi, 2014a). Conductive composite membrane-phytic acid (PA) doped polyaniline (PANI)/cellulose acetate (CA) (PANI-PA/CA) was used as adsorbent for chromium removal by Renjie et al. (R. Li, Liu, & Yang, 2014). PANI nanocomposites were prepared by in situ oxidative polymerization of aniline in acidic medium using ammonium persulphate as initiator in the presence of natural silica (PANIS), acid treated natural silica (PANISA), fiber glass (PANIFG), and poly(ethylene terephthalate) powder from waste bottles (PANIPET) for removal of Chromium (Najim & Salim, 2014).

The Ethyl celluloses (ECs) modified with PANI (PANI/ECs) prepared by homogeneously mixing the EC and PANI formic acid solutions showed superior Cr^{+6} removal performance to that of pure EC (Qiu, Xu, Sun, Yi, et al., 2014). The organic-inorganic hybrid material of PANI/Mg/Al layered double hydroxides (PANI/LDHs) was fabricated through in situ oxidative polymerization by Kairuo Zhu et al. (Zhu, Gao, Tan, & Chen, 2016). Magnetic mesoporous carbon incorporated with polyaniline (PANI-Fe/OMC) was developed for enhanced adsorption and reduction of Cr^{6+} to Cr^{3+} by Yang et al. (Yang et al., 2014).

Nano sized polyaniline and its composites have recently been investigated for its potential for removal of chromium. One-dimensional polyaniline (1D PANI) nanowire/tubes with rough surface were prepared by a simple chemical oxidation method by Guo et al. to remove Cr6+ rapidly and effectively in one step from aqueous solution by reducing Cr6+ to Cr3+ (Guo et al., 2011). Three nanostructured PANIs with different morphologies, including nanofibers, nanotubes and nanosheets, have been successfully synthesized using MnO_2 with tunable morphologies as the reactive templates by Tian et al. for removal of chromium (Tian et al., 2016). Polypyrrole-sepiolite nanofibers were prepared by in situ chemical oxidation polymerization in the presence of sepiolite for removal of chromium by Chen et al. (Chen, Hong, Xie, Li, & Zhang, 2014). Polyacrylonitrile/polyaniline core/shell nanofibers were prepared by Wang et al. for removal of Cr^{6+} (Jianqiang Wang et al., 2013). Wen et al. synthesized a core-shell structure of polyaniline/hydrogen-titanate nanobelt for removal of Cr^{6+} (Wen et al., 2016). The behavior, mechanism and kinetics of toxic hexavalent chromium Cr^{6+} removal by magnetic polyaniline nanocomposites from different pH solutions were reported by Hongbo Gu et al. (Gu et al., 2012). Cr^{6+} can be removed fast by PANI/CF with the reduction of Cr^{6+} to Cr^{3+} by PANI was observed by Bin Qiu et al. (Qiu, Xu, Sun, Wei, et al., 2014).

Zhang et al. synthesized PANI@GO nanocomposite with adsorption capacity of 1149.4 mg/g for Cr^{6+}, which is one of the highest capability of today's nanomaterial (S. Zhang et al., 2013).

In general during the investigation of the adsorption process of various forms of PANI for chromium, researchers have reported conventional Langmuir isotherm and pseudo second order as better fits for polyaniline based adsorbents and monolayer adsorption. Tang et al in their study on the use of polyaniline–magnetic mesoporous silica composite probably suggested that the adsorption was mainly driven by the molecular interaction between Cr^{6+} ions and the protonated PANI on the adsorbent, which was in consistence with their result from adsorption kinetic study (Tang et al., 2014).

M.K. Kim et al. (Kim et al., 2015) discussed that removal of chromium follows both pseudo second and first order kinetics onto chitosan functional gel included with multiwall carbon nanotube and substituted polyaniline, They also reported deviation from Langmuir monolayer adsorption and fitting of Freundlich isotherm.

Rajeev Kumar et al in their study on the use of DBSA doped polyaniline/multi-walled carbon nanotubes composite for removal of Cr^{6+} from aqueous solution (R. Kumar et al., 2013) suggested that the adsorption was heterogeneous, multilayer and controlled through a boundary layer affect the equilibrium isotherm and kinetic results. The functional groups present on the

surface of adsorbent mainly, amine or imine groups of polyaniline and exposed surface and internal porous structure sites were mainly responsible for the adsorption of Cr^{6+}. However they did not study any multilayer isotherm model except for Freundlich model which assumes a heterogeneous adsorption surface.

Our objective was thus to synthesize nanopolyaniline and reinvestigate the adsorption potential and adsorption mechanism for chromium removal by spectoscopic techniques and kinetic as well as isotherm models.

4.2 Materials and Methods.

4.2.1 Materials

All the reagents used were of AR grade. Aniline [Renkem, India], Ammonium persulphate and Hydorchloric acid (Lab India, INDIA) were used as such without further purification.

4.2.2 Synthesis of Adsorbent Polyaniline-(PANI)

Polyaniline was prepared adopting the method of Stejskal and Gilbert (J. Stejskal & Gilbert, 2002) with slight modifications. 100 mL of 0.25M of aqueous solution of Ammonium persulfate $(NH_4)_2S_2O_8$ and 0.20M solution of aniline was dissolved in 100mL of 1M HCl at 5°C. Polymerization was allowed to proceed overnight in a refrigerator. The green precipitate that was formed was separated by filtration, washed with 1M HCl followed by acetone until clear filtrate was obtained. The precipitate was dried in a vacuum oven at room temperature (30°C) for 6 hours. Green colored PANI was obtained which was investigated for its adsorption potential towards Cr^{6+}. The synthesized PANI was then characterized by various techniques such as XPS, ESR, FT-IR, Raman as well as Absorption and Emission Spectroscopy as described in sections 3.2.8.1 to 3.2.8.11.

4.2.3 Preparation of metal solution

Stock solutions of Cr^{6+} and working solutions were prepared as described in section 2.2.3 of Chapter 2

4.2.4 Batch sorption Experiments

Batch sorption experiments were performed as described in section 2.2.4 of Chapter 2 using PANI as adsorbent wherein the remaining concentration of Cr^{6+} was determined by Inductive Couple Plasma Instrument. Isotherm, kinetics and thermodynamic studies were done as described in chapter 2 using PANI as adsorbent.

4.2.5 Desorption

For desorption studies, 0.05g of PANI preloaded with known amount of Cr^{6+} was equilibrated with 25 ml solutions of 0.1 M of NaOH, H_2SO_4, HCl and HNO_3 for 120 min. The contents of the flasks were filtered and the chromium content in the filtrate was determined by ICP. Three consecutive adsorption-desorption cycles were carried out to test the reusability of PANI.

4.3 Results and discussion

4.3.1 Zeta Potential Analysis

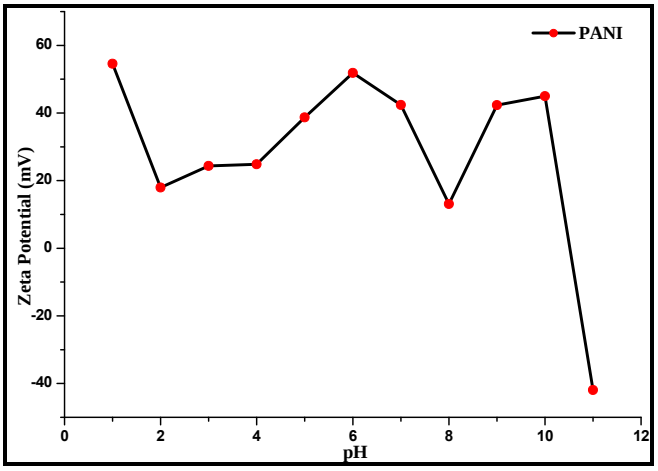

Figure 4.2 Zeta Potential of PANI

The values of zeta potential for PANI were positive at all pH conditions from 1 to 10 (Figure 4.2), with a pZc value of 10.3 indicating that PANI backbone acquired positive charge and was a polycation. This was a consequence of doping in the presence of adequate H^+ ions where in protonation of the nitrogen atoms of the polymer matrix occurred. The fact that the positive charges are not neutralised even at pH 10 indicates the very high doping level of PANI sample (Ležaić, Bajuk-Bogdanović, Radoičić, Mirsky, & Ciric-Marjanovic, 2016).

4.3.2. Elemental Analysis and Surface Properties (CHNS)

Elemental analyses of PANI were conducted by CHN microanalysis and SEM EDX techniques and are presented in Table 1 and SEM images in Figure 4.3.

Table 4.1 CHN microanalysis

	PANI			**PANI-Cr^{6+}**		
Element	**Weight%**	**Atomic%**	**CHN**	**Weight%**	**Atomic%**	**CHN**
Carbon	70.59	73.68	52.1734	43.93	55.84	39.4373
Nitrogen	9.42	16.53	9.337	1.83	1.99	6.5525
Hydrogen			4.5927			4.1437
Sulfur			0.2856			0
Oxygen	4.63	3.92		39.73	37.91	
Chloride	15.36	5.87				
Chromium				14.51	4.26	

The comparable percentages of nitrogen in both EDX and CHN analyses in PANI indicated the presence of the nitrogen backbone in the polymer chain (Zhao, Zhang, Yu, & Tang, 2016). It is not so in the case of PANI-Cr due to presence of chromium. In general, the C/N ratio is ~6 for aniline units in PANI.

Surface area, pore volume, and pore diameter of the composite biosorbent were determined with a BET instrument by means of adsorption of ultra-purity nitrogen at -196 °C.

The surface area of the Polyaniline adsorbent material obtained from N_2 adsorption−desorption study was found to be 37.6716 m^2/g. A pore size of 149.6430 Å corresponding to a maximum pore volume of 0.08255 cm^3/g was obtained from the Barrett-Joyner-Halenda (BJH) pore size distribution curve.

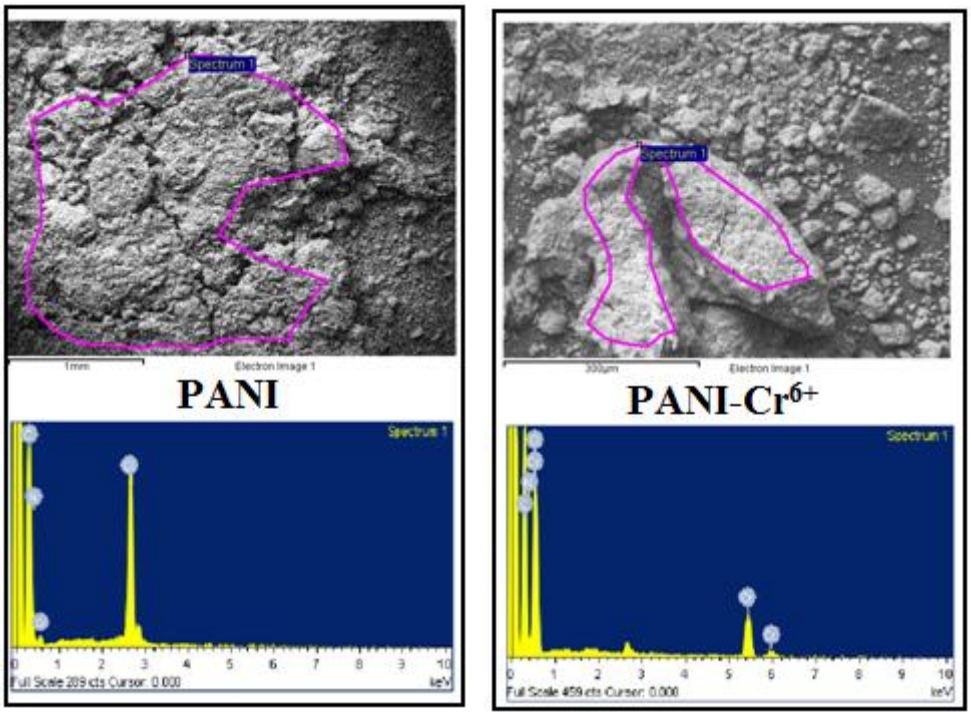

Figure 4.3 SEM / EDAX of PANI and PANICr^{6+}

4.3.3 TEM Analysis

It is seen from PANI TEM image that polyaniline spheres of size 25-45 nm as well as nanofibers seem to have formed.

PANI

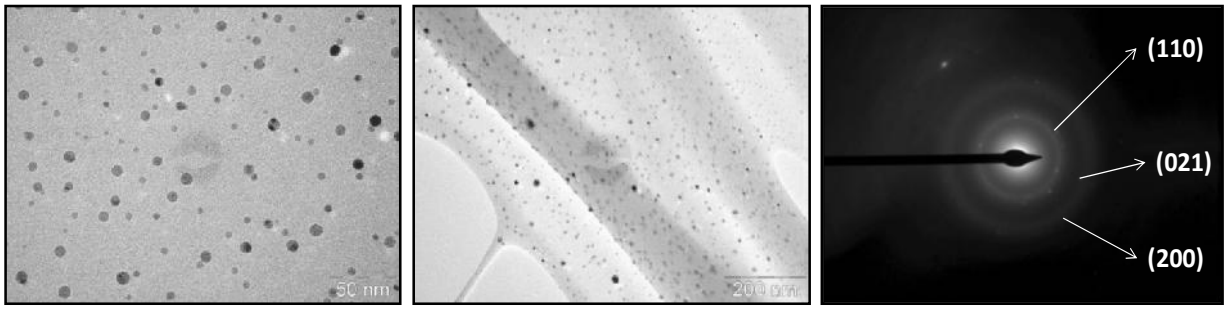

PANI-Cr

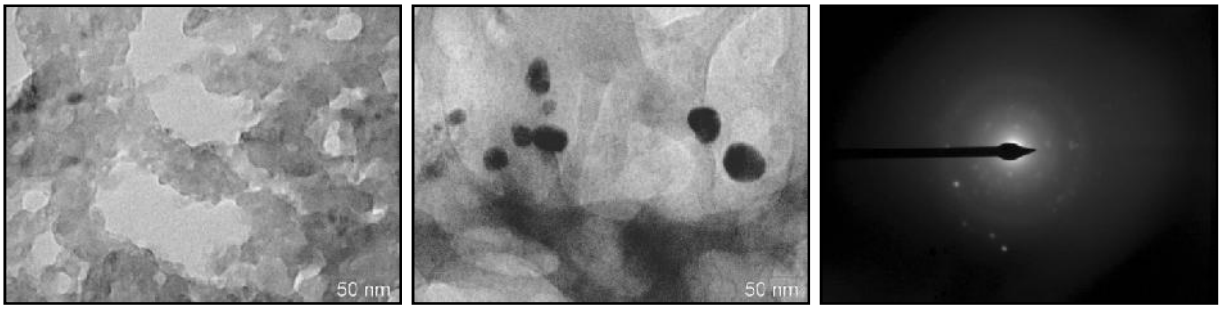

Figure 4.4 TEM images of PANI and PANI-Cr^{6+}

A Polymeric network is formed after chromium adsorption in which nano chromium as hydroxy species with irregular morphology resulted from adsorption of chromium and there was loss of crystallinity.

4.3.4 UV–Vis Analysis

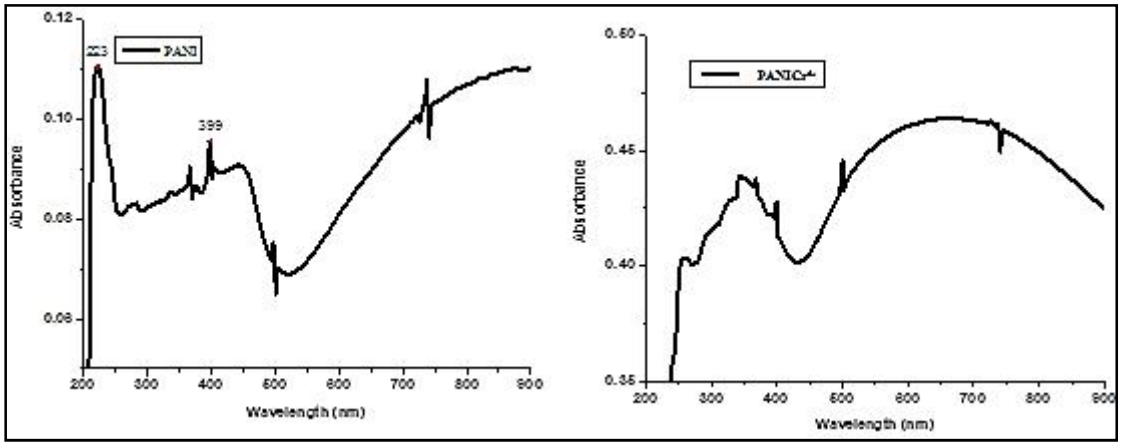

Figure 4.5 UV–Vis spectra of PANI and $PANICr^{6+}$

The absorption peak observed at 330 nm in PANI (Figure 4.5) is probably due to the π–π* transition in the benzenoid ring (Farhadi, Zebhi, Moghadam, Es'haghi & Ashassi-Sorkhabi, 2014), while the absorption peak at 399 nm can be assigned to aniline oligomeric intermediates containing phenazine-like structures (Ding et al., 2010; Fernandez & Pizarro, 1997; Galasso, 2008) viz. the π- π* transition of the benzenoid rings and polaron bands in emeraldine salt state (Hong, Hwang, Yoon, & Yang, 2015). The broad shoulder at around 471 nm is due to polaron-

π* transition (Colomban, Folch, & Gruger, 1999; Epstein et al., 1987; Folch, Gruger, Régis, & Colomban, 1996; Watanabe, Mori, Iwasaki, Nakamura, & Niizuma, 1987). The pi-bipolaron transition of emeraldine salt is associated with absorption at 770 nm., The plateau at about 800–1000 nm indicates emeraldine salt state of PANI (Hong et al., 2015). The broadening extended towards the near infra-red region is characteristic to that of highly conductive polymers indicating increased concentration of polarons leading to the easier delocalization of π-electrons (Dhand, Singh, Arya, Datta, & Malhotra, 2007).

In PANI-Cr the broad absorption band at ~600 nm is due to the donor–acceptor interaction of quinonoid ring (Farhadi et al., 2014) and is again indicative of conductive emeraldine salt.

4.3.5 Photoluminescence Analysis

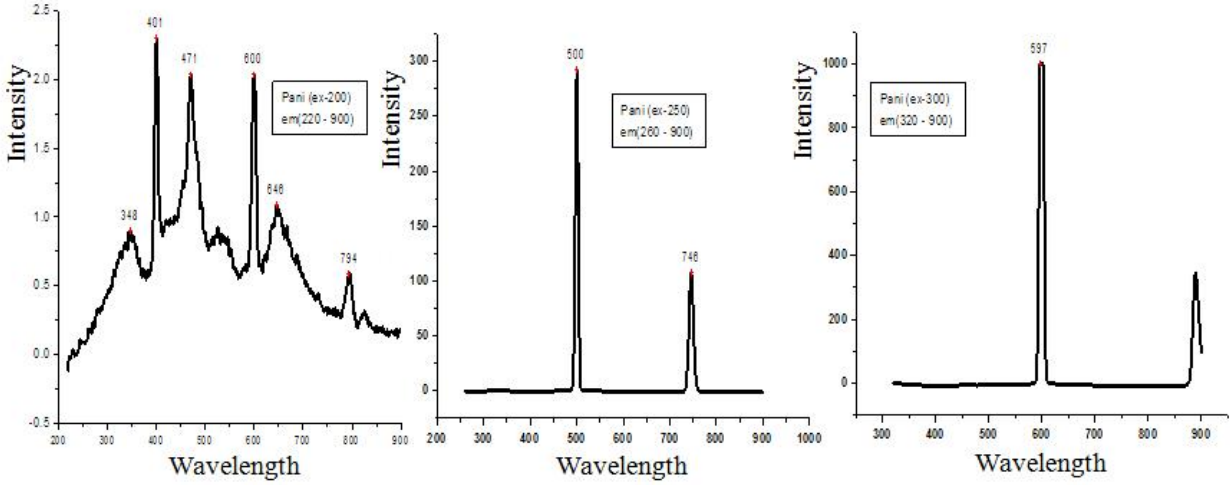

Figure 4.6 Photoluminescence spectra of PANI

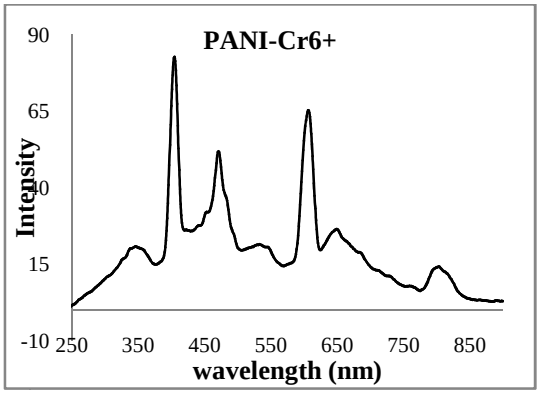

Figure 4.7 Photoluminescence spectra of PANI-Cr^{6+}using excitation wavelength 225nm

The emission peak at 348 nm in PANI and PANICr^{6+} (Figure 4.7) can be attributed to π→π* transition of benzenoid unit while the peak at 401 nm can be attributed to fully reduced form of benzenoid species in leucoemeraldine form of PANI (Collins & Goldsmith, 1981; Shimano & MacDiarmid, 2001).The emission at 471 nm can be attributed to $S_0 \rightarrow S_1$ transition

and various vibronic side bands at lower energy are also observed in PANI (Ram, Mascetti, Paddeu, Maccioni, & Nicolini, 1997) due to presence of reduced qinonoid unit in emeraldine salt form if present adjacent to benzenoid units when excited at 225 nm. A shoulder at 500 nm is indicative of quinoid unit in PANI and PANICr^{6+}. The emission peaks in ~500-600 nm range confirms the benzenoid and quinoid units in PANI and PANICr^{6+} specifically arranged in a proper order amenable for the formation of excitons and increase in the delocalization length of a singlet exciton (Shimano & MacDiarmid, 2001).

4.3.6 FTIR Analysis

Figure 4.8 shows the FTIR spectra of PANI and PANICr^{6+}.The characteristic peaks observed in the FT-IR spectra and their assignments are given in Table2. The Characteristic Cr-O stretching is observed in PANI-Cr.

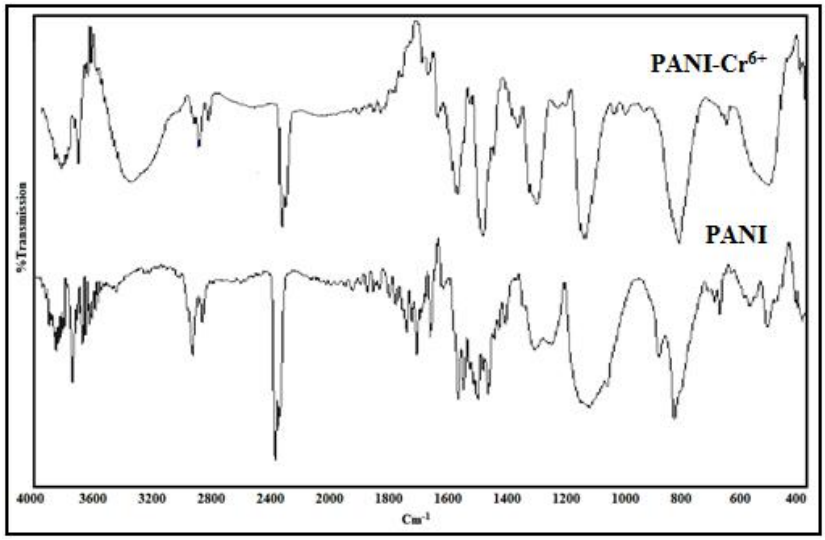

Figure 4.8 FTIR Spectra of PANI and PANICr^{6+}

Table 4.2 FTIR analysis of PANI and PANI-Cr^{6+}

PANI	PANICr^{6+}	Inference
3854, 3747, 3675	3859, 3747, 3389	N-H Stretching vibration
2929,2857, 2358, 2330	2935, 2851, 2364, 2330	-CH stretching vibration in –CH and –CH_2
1681, 1650	1644	-NH_2 bending vibration
1493, 1457	1499	stretching vibrations of the benzenoid ring
1558,	1583	stretching vibrations of the quininoid ring (Q)
1395	1379	C- N deformation mode
1241		C=N stretching band of an aromatic amine
1297	1314	C–N stretching of secondary aromatic amine
1048	1051, 1009	N=Q=N stretching band Q refers to the quinonic type rings
1113		aromatic C–H in-plane bending
	1152	vibrational mode of benzenoid–NH+ = quinoid structure
872	ND	ring symmetric stretching vibration characteristic of para-disubstituted benzene
822	830	C–H out-of-plane bending deformation of benzene ring
	668, 525	Cr–O stretching vibration

(Dhand et al., 2007; Kousalya, Rajiv Gandhi, & Meenakshi, 2010; J. S. Wang, Peng, Yang, Liu, & Hu, 2011; Zuo & Balasubramanian, 2013)

4.3.7 Raman Analysis

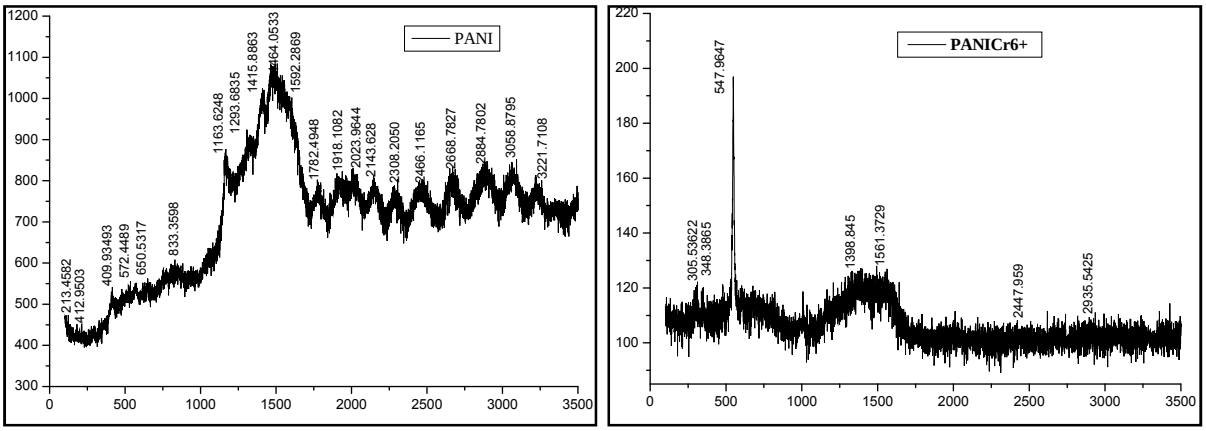

Figure 4.9 Raman Spectra of PANI and PANICr^{6+}

Figure 4.9 shows the Raman spectra of PANI and PANI- Cr. The characteristic bands of emeraldine salt were observed in the Raman spectra of PANI samples In pristine PANI sample, the Raman peaks appear at ∼1163 cm^{-1}, ∼1293 cm^{-1}, ∼1464 and 1592 cm^{-1}, corresponding to the vibrations of C-H benzenoid or quinoid stretching, C-N benzenoid stretching, C=N quinoid stretching and C=C quinoid stretching, respectively (Pei et al., 2014; Xia et al., 2012). The band at 1592 cm^{-1} and 1562 cm^{-1} in pristine PANI and PANI-Cr can be attributed to the C=C deformation of semiquinoid rings and C=C stretching in quinoid; the band at 1415 cm^{-1} can be assigned to the C=N stretching of semiquinoid rings; the peak at 1399 cm^{-1} in PANI-Cr^{6+} is characteristic of the N-H bending deformation band of the protonated amine; the band at 833 cm^{-1} is attributed to the in PANI ring deformation in Q-ring; the peak at 650 cm^{-1} is associated with amine deformation in B; the band at 409 cm^{-1} can be assigned the out-of-plane C-H wagging in the bipolaronic and CNC torsion of polaronic structures in Q-ring (Baibarac et al., 1999; Izumi, Andrade, & Temperini, 2008; Jain & Annapoorni, 2010; Luo et al., 2011; Pereira Da Silva, De Faria, Cordoba De Torresi, & Temperini, 2000). The intensity of the bands is reduced in Cr-PANI. Characteristic peaks of Cr are observed at 305.53, 348.38,548 cm^{-1}. The band at 548 cm^{-1} is of A1g symmetry while the other two are Eg vibrations.

(other references used for asssignments-Ciric -Marjanovic, Gordana Trchova & Stejskal, 2008; Ležaić et al., 2016; Trchova, Moravkova, Blaha, & Stejskal, 2014; Trchova, Moravkova, Dybal, & Stejskal, 2014).

4.3.8 TGA and DSC

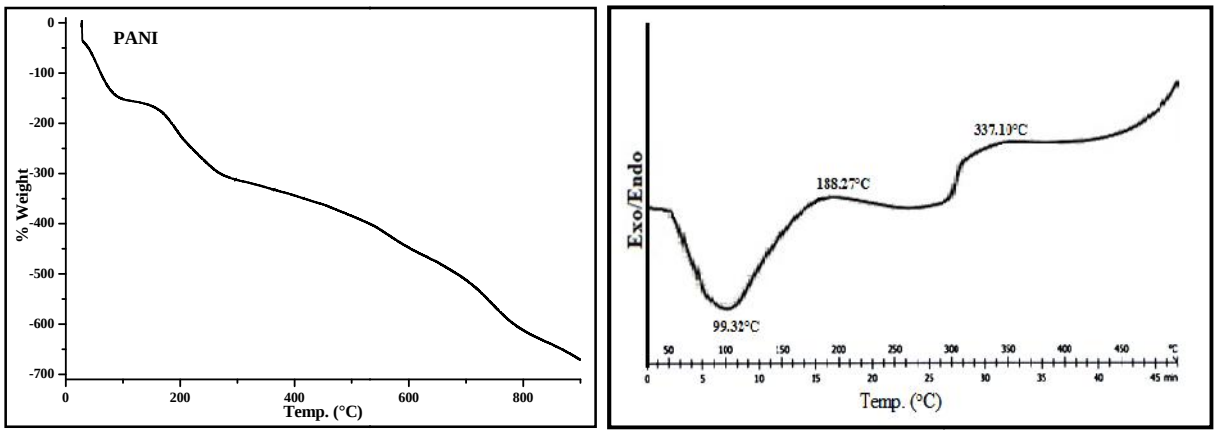

Figure 4.10 TGA and DSC analysis of PANI

The first mass loss between 25°C to 100°C is attributed to loss of water contained in the polymer. The weight loss at 100-200°C could be attributed to further loss of moisture and dopant anion. This is followed by continuous weight loss due to decomposition of PANI.

DSC analysis of PANI is characterized through a broad endothermic transition, starting at approximately 52°C and centered at approximately 92°C corresponding to its glass transition temperature (Figure 4.10) (Srinivas, Srinivasu, Kavitha, Narsimlu, & Siva Kumar 5, 2012). Exothermic peaks at 188°C and 337°C are due to oxidative degradation of PANI.

4.3.9 XRD Analysis

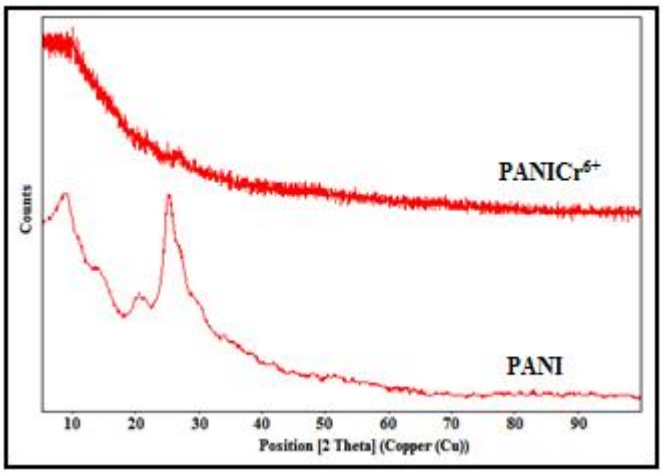

Figure 4.11 XRD spectra of PANI and $PANICr^{6+}$

The pristine PANI exhibits four peaks located at ~9.5°, ~ 15.1°, ~20.1° and ~25.3° (N. Li et al., 2016) corresponding to the diffractions of (001), (010), (100) and (110) crystallographic Planes of PANI in its emeraldine salt form. A peak at around 9.5° appears in long chain polyanilines in highly ordered pernigraniline form of PANI. The peak at 2θ 15.1° is attributed to the periodicity parallel to the polymeric chain in emeraldine salt (Sonmez, Sonmez, Shen, & Wudl, 2004). The peak centered at a 2θ value of 20.1° is due to emeraldine base. The reflections

at 25.3° are the most intense which arise from the periodicity perpendicular to the polymer chain and from the crystallinity of polymer. (Du, Zhang, Han, Liu, & Wan, 2005) The d-spacing of 3.45 Å associated with the diffraction peak at 25.3° corresponded to the face-to-face inter chain stacking distance between phenyl rings. With increased protonation, the intensity of diffraction peak at 2θ value of 20.1° is less while the peak at 25.3° is of increased intensity. The diffraction peaks indicate that PANI polymer is partially crystalline but predominantly amorphous.

The XRD pattern of PANI after adsorption of Cr^{6+} exhibits only one broad hump indicating that PANI has become completely amorphous. The spectra suggested the formation of nanoparticles (Ayad & Zaghlol, 2012).

4.3.10 ESR Analysis

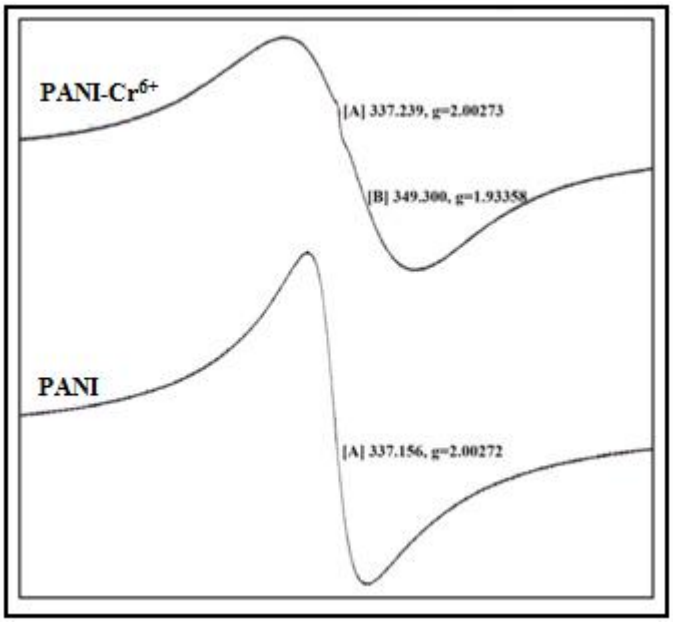

Figure 4.12 ESR Spectra of PANI and PANICr^{6+}

Pristine PANI shows an ESR signal with a g value of 2.00272 (Figure 4.12) indicating the presence of polaron in PANI. Poly [semi-quinone radical cations] or polarons are present as charge carriers.(Karim, Lee, Park, & Lee, 2005). This value is characteristic of emeraldine salt. However a slight shift from, ge = 2.00273 suggests that the spins in PANI are delocalized over some repeating units.(Krinichnyi, Roth, Schrodner, & Wessling, 2006).The g value of Cr is related to exchange interactions between the bound chromium species (Tsukerblat, Kuyavskaya, Fainzilberg, & Belinskii, 1984).

4.3.11 XPS Analysis

The pristine PANI and PANI after equilibration with chromium were characterized by XPS and the observed main peaks are tabulated in Table 4.3

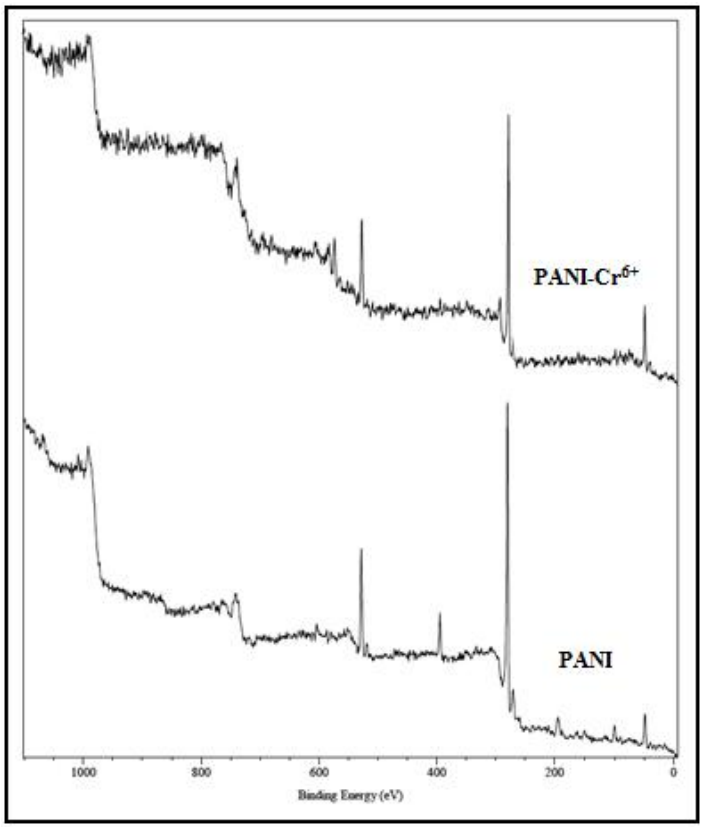

Figure 4.13 XPS spectra of PANI and PANI-Cr^{6+}

Table 4.3 XPS analysis of PANI and PANI-Cr^{6+}

Sample name		Binding Energy (eV)	FWHM eV	Area	Percentage
PANI	C 1s	284.604	2.229	27701.2	76.0
	C 1s	286.283	2.241	8765.8	24.0
	O 1s	532.776	2.853	19529.8	100.0
	N 1s	399.253	2.622	5106.6	74.4
	N 1s	401.147	3.141	1757.3	25.6
	Cl 2p	197.329	2.391	1771.6	36.5
	Cl 2p	200.216	2.371	1273.1	26.2
	Cl 2p	199.156	2.317	1163.6	24
	Cl 2p	201.862	1.94	644.2	13.3
$PANICr^{6+}$	C 1s	284.604	2.019	14035.9	71.3
	C 1s	285.785	2.378	5650	28.7
	O 1s	531.474	2.805	13392.5	73.9
	O 1s	533.13	2.732	4728.1	26.1
	N 1s	398.658	1.285	273.7	31.7
	N 1s	399.677	1.204	346.8	40.2
	N 1s	400.724	1.014	241.6	28
	Cr 2p3/2	577.226	3.055	5487.1	44
	Cr 2p1/2	586.469	2.993	2985	23.9
	Cr 2p3/2	579.785	3.384	2483.5	19.9
	Cr 2p1/2	589.04	2.948	1513.5	12.1

C 1s : The peak at binding energy 284.6 eV is attributed to the neutral C-C or C-H bonds the backbone of the polymer. The 286.2 eVpeak can be attributed to the carbon atoms bonded to polaronic-type and bipolaronic-type nitrogen atoms. The peak at 285.7 eV in PANI-Cr is attributed to C-N/ C=N (Lekha, Subramanian, Yi, Dhanuskodi, & Padiyan, 2010).

N 1s : In PANI the 399.2eV peak is assigned to benzenoid amine, the 401.1eV peak assigned to protonated nitrogen atoms with iminium ion. (Yue & Epstein, 1991). The N1s XPS data of PANI-Cr could be deconvoluted into 3 peaks, located at 398.6eV, 399.7 eV and 400.7 eV. The first peak is assigned to quinoid imine, the second one to benzenoid amine, the third one to protonated nitrogen atoms with iminium ion(Yue & Epstein, 1991). The shift to higher binding energy as compared to PANI is indicative of interaction of polyaniline with chromium. The Cr^{6+} is reduced to Cr^{3+} by the oxidation of benzenoid amine to quinoid imine

Cr 2p : The binding energy peaks at 577.2 and 579.7eV correspond to Cr-OH/Cr-Cl of trivalent hydroxy species of chromium or chloride (Ithurbide, Frateur, Galtayries, & Marcus, 2007; Murphy, Tofail, Hughes, & McLoughlin, 2009; Park, Yun, & Park, 2008).

Cl 2p : The Cl 2p peaks are fitted with spin-orbit doublets (Cl $2p_{1/2}$ and Cl $2p_{3/2}$, with area ratio ~1:2 and BE separation of ~1.6 to 1.8 eV). The Cl $2_{p3/2}$ component at ~197.3 eV represents anionic Cl while the peak around 200.2 eV can be attributed to covalently bonded chlorine (Qaiser, Hyland, & Patterson, 2012).

O1s spectra: The presence of oxygen is due to superficial oxidation or presence of water (Golczak, Kanciurzewska, Fahlman, Langer, & Langer, 2008).

4.4. Adsorption-Desorption Studies

4.4.1 Effect of pH

The effect of pH on the adsorption process is presented in Figure 4.14 wherein the adsorption was determined over the pH range 1-11 using 0.05 g PANI and 50 ppm chromium solution. Chromium can exist in various ionic forms at different pH values. Hence, the initial solution pH strongly influences its adsorption It was observed that maximum adsorption of Cr^{6+} occurred at pH 2–6 where zeta potential was highly positive and decreased at higher pH values.

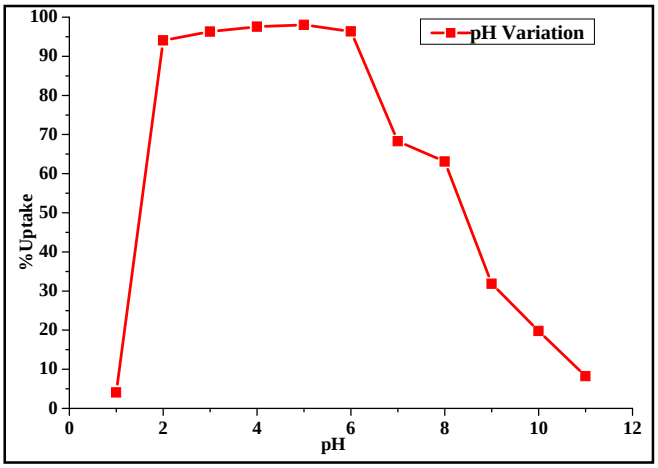

Figure 4.14 Effect of pH:

Volume = 25 ml, Amount adsorbent = 0.05 g, (Cr^{6+})= 50 ppm: pH = 1 to 11, contact time =4 h, Temperature = 30°C.

. Cr^{6+} predominantly exists in its anionic $HCrO_4^-$ form at pH 5. The state of amine/ imine groups of PANI is also pH dependent and are protonated resulting in electrostatic interactions between the protonated amine/imine groups of PANI and negatively charged Cr^{6+}.

4.4.2 Effect of Adsorbent Dose

The effect of sorbent dose was also investigated (Figure 4.15). Different amounts (0.01–0.1 g) of sorbent were suspended in 25 mL Cr^{6+} solution (50 ppm) under optimized conditions. It was observed that the adsorption percentage of Cr^{6+} onto the PANI increased with increasing adsorbent concentration and reached saturation limit at 0.05 g. This could be due to greater surface area with increased adsorbent dose.

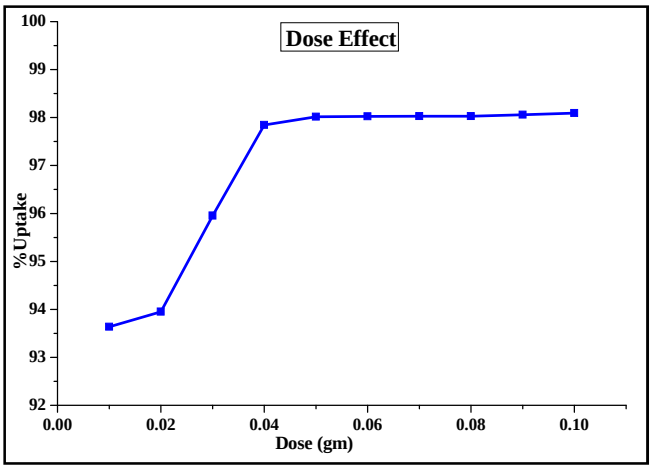

Figure 4.15 Effect of Dose: Volume = 25 ml, Dose = 0.05 g to 0.1g, (Cr^{6+}) = 50ppm

pH = 5, contact time =4 h, Temperature = 30°C

4.4.3 Effect of Concentration Variation

The effect of metal ion cocentration on the uptake behavior of PANI was studied in the concentration range 10-1000 ppm of the metal ion (Figure 4.16). The percent uptake content was found to decrease with increase in concentration of Cr^{6+}. However q_e would increase with increase in the initial concentration of Cr^{6+} solution.

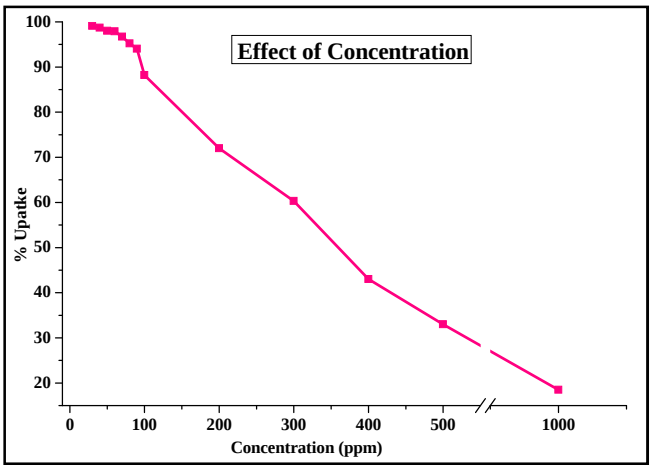

Figure 4.16 Effect of Concentration:

Volume = 25 ml, Amount adsorbent = 0.05g, (Cr^{6+}) = 50ppm to 1000ppm pH = 5, contact time = 4 h, Temp. = 30°C

The data was fitted with isotherm models (mentioned in section 2.2.5 of chapter 2) and isotherm constants for the adsorption of Cr^{6+} by PANI are presented in Table 4.4. The adsorption data for PANI gave reasonably high correlation coefficient values for all the models studied. From the correlation coefficients (Table 4.4), the Freundlich model simulates the experimental data better than the Langmuir model suggesting that monolayer adsorption was not taking place on PANI. The Freundlich constant, n was more than unity implying that the adsorption intensity was favorable over the entire range of concentrations studied and also suggests a interactive nature for the Cr^{6+} adsorption process (Kim et al., 2015). The maximum removal capacity of Cr^{6+} by PANI calculated from Langmuir isotherm model was 91.32 mg/g.

The fitting of Temkin model indicated favorable adsorption of Cr^{6+} onto adsorbent under study. The high regression values for Halsey model suggest multilayer adsorption. The low fitting of the Langmuir adsorption isotherm of Cr^{6+} on PANI could be due to the low saturation of the adsorbent surface of PANI. This has been reported to occur on the surface of non-porous or macropore adsorbents. Upon completion of the monolayer adsorption process, the second layer may begin to form with the increase in the relative pressure of the adsorbate (the increase in the concentration of Cr^{6+} relative to the saturation vapor pressure). More and more layers can form (Gao, Chen, Tan, Xu, & Zhu, 2016).

The negative values of n_{FH} and low values of K_{FH} (Table 4.4) of FH isotherm implied that the Flory-Huggins model cannot be used to describe the adsorption data. The high correlation coefficient of Elovich isotherm further suggested multilayer adsorption.

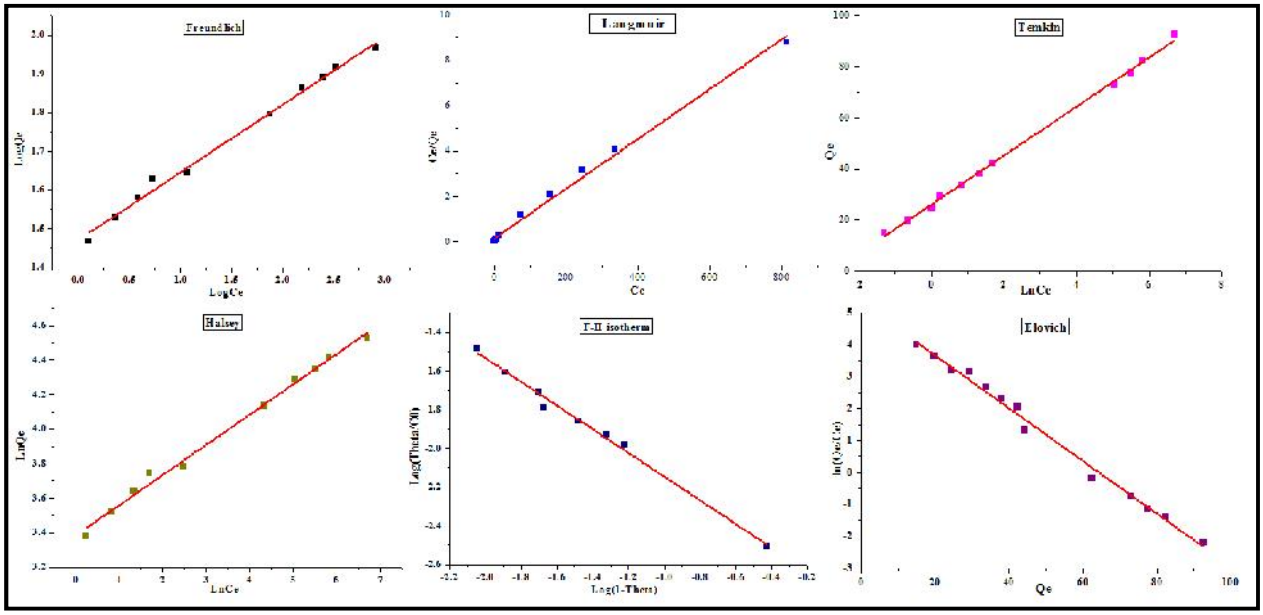

Figure 4.17 Isotherm linear Plot for Cr^{6+} adsorption on PANI

Table 4.4 Isotherm constants for Cr^{6+} adsorption on PANI

Isotherms	**Constants**				
Freundlich	K_f ($L.g^{-1}$)	N	r^2	SD	
	29.4985	5.6983	0.9937	0.0151	
Langmuir	KL ($L.mmol^{-1}$)	q_m ($mg.g^{-1}$)	ΔG ($kJ.mol^{-1}$)	r^2	SD
	0.0728	91.3242	-6.8085	0.9943	0.2031
Temkin	BT	$-\Delta H$ ($kJ.mol^{-1}$)	KT ($L.mmol^{-1}$)	r^2	SD
	9.6083	0.0532	15.0093	0.9981	1.2683
Halsey	k_H ($L.g^{-1}$)	n_H	r^2	SD	
	29.4988	-5.7081	0.9937	0.0348	
F-H isotherm	N_{FH}	r^2	SD	K_{FH}	
	-0.6126	0.9923	0.0293	0.0017	
Elovich	qm ($mg.g^{-1}$)	K_E ($L.mmol^{-1}$)	r^2	SD	Lnq_m
	12.1080	16.8497	0.9917	0.2039	2.4939

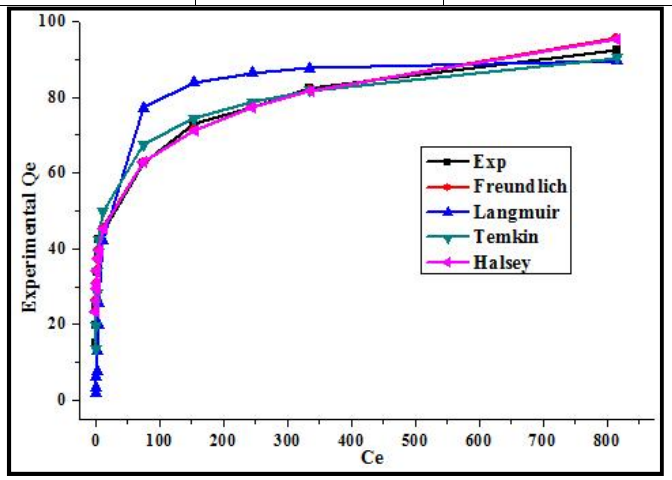

Figure 4.18 Back-calculated isotherm models for Cr^{6+} adsorption on PANI

4.4.4 Sorption Kinetics

The time dependent Cr^{6+} adsorption was studied on PANI (Figure 4.19). The experimental results show increase in the Cr^{6+} removal with time.

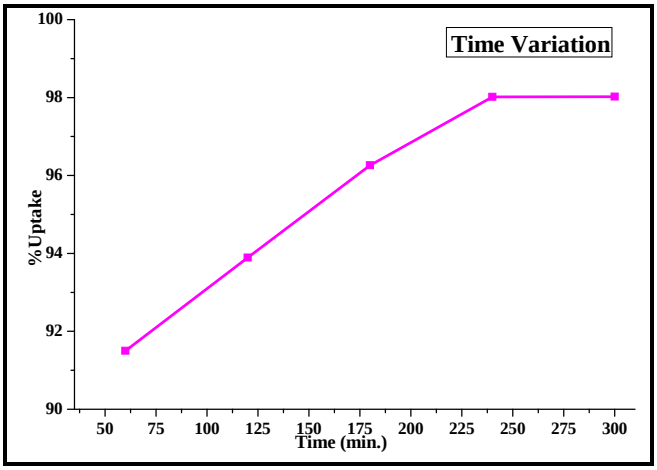

Figure 4.19 Effect of Time

Volume = 25 ml, Amount adsorbent = 0.05 g, (Cr^{6+}) = 50 ppm: pH = 5, contact time=5 h, Temp. = 30°C

It is observed that the rate of uptake is very high initially with around 91% of Cr^{6+} being removed in about 60 minutes and equilibrium is achieved in 240 minutes. The removal rate is high initially due to the presence of free binding sites on PANI which gradually get blocked with time and hence there is decrease in rate of adsorption. The order of adsorption of chromium was investigated by fitting the kinetic data to different kinetic models (section 2.2.6 of Chapter 2). The rate constants for different kinetic models are presented in Table 4.5. The correlation coefficients for pseudo second order model were found to be high and the calculated qe values were closer to those obtained experimentally. This indicated that surface complexation may be the rate limiting step which involves valence forces through sharing or exchanging of electron between adsorbent and adsorbate.

For pseudo first order kinetics fitting, the value of r^2 was better than pseudo second order model but qe values were very much lesser than those observed from experiment. The liquid film diffusion and Elovich equations were used to determine the mass transport and chemical adsorption mechanism of Cr^{6+}. The reasonably good correlation coefficients confirm the existence and importance of diffusion-control in the transport/adsorption mechanism for Cr^{6+} adsorption by PANI.

The plot of q_t versus $t^{1/2}$ did not pass through origin suggesting that intraparticle diffusion was not the only rate controlling step but some degree of the boundary layer diffusion also controlled the adsorption process and that the overall rate of the metal adsorption process appeared to be controlled by more than one-step. The reasonably good correlation coefficient for

Bangham equation indicated that the diffusion of Cr^{6+} into the pores of the adsorbents under study also controlled the adsorption process.

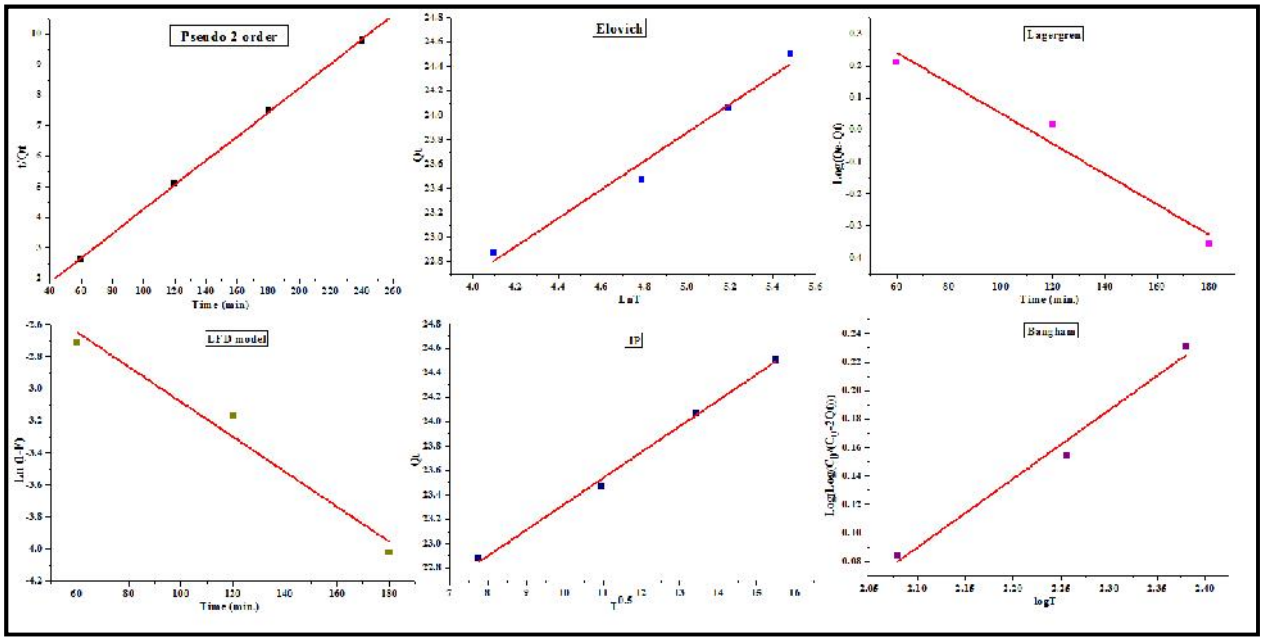

Figure 4.20 Kinetics Linear Plot of Kinetic models for adsorption of Cr^{6+} on PANI

Table 4.5 Kinetic constants for Cr^{6+} adsorption on PANI

Isotherm	**Constants**			
Experimental q_t (mg/g)	**24.51**			
Pseudo 2 order	q_t (mg/g)	K	r^2	SD
	25.126	0.0056	0.9997	0.0623
Elovich	B	Alpha	r^2	SD
	0.8565	3.2E+15	0.9788	0.12643
Lagergren	q_e (mg/g)	K	r^2	SD
	3.351	0.0109	0.9705	0.0701
Liquid film diffusion model	K_{fd}	r^2	SD	
	0.0109	0.9705	0.1614	
Intraparticle	K	I	r^2	SD
	0.2125	0.9972	0.0459	0.041
Bangham	K_m	Alpha	r^2	SD
	-53.168	0.4826	0.9847	0.0128

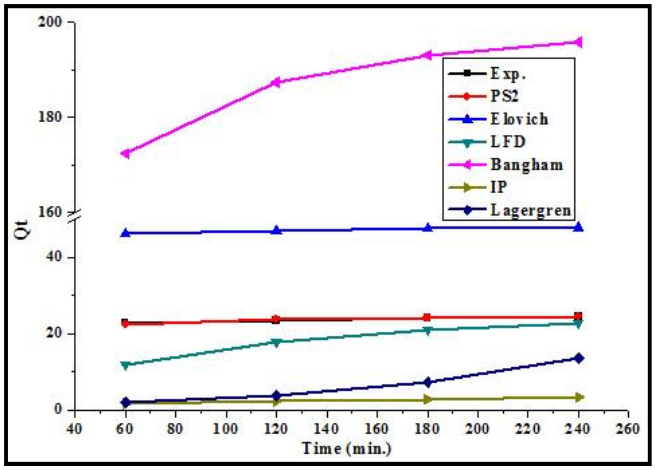

Figure 4.21 Kinetics model fits for PANI

As the adsorption kinetics and isotherm follow less familiar relationships such as the Lagergren, LFD as well as elovich kinetic models and Freundlich and Halsey isotherm models the mechanism of uptake of chromium seems to be complex and multilayered.

4.4.5 Effect of Temperature

The metal uptake for PANI decreased with increase in temperature from 30°C to 70°C (Figure 4.22) indicating that the metal uptake onto PANI was dependent on temperature and that the adsorption process was exothermic. This decrease in the uptake capacity with increasing the temperature might be due to decreasing the surface activity that leads to the decrease in the thickness of the boundary layer which increases the tendency of the metal ion to escape to the solution.

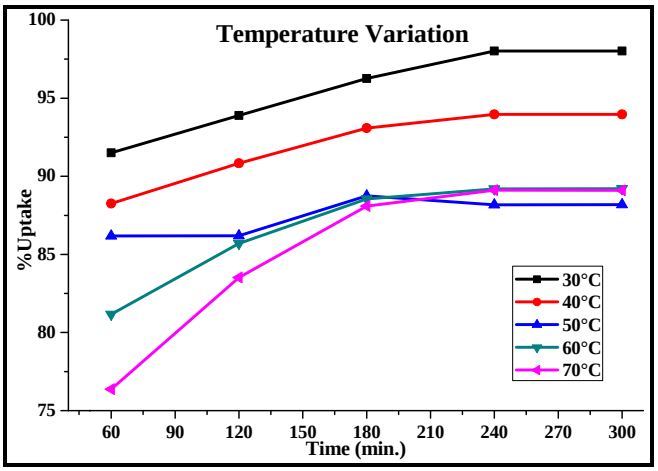

Figure 4.22 Temperature Variation: Volume = 25 ml, Amount adsorbent = 0.05 g (Cr^{6+}) = 50 ppm effect of temperature: pH = 5, contact time =1-5 h, Temp. = 30-70°C.

The free energy change during the adsorption process was negative for the experimental range of temperatures (Table 4.6) suggesting chemisorption to be the mechanism of adsorption. The negative value of enthalpy change indicated that the adsorption was physical in nature not

involving strong forces of attraction and is exothermic. The negative entropy change corresponded to decreasing system randomness at the solid-liquid interface during the adsorption process.

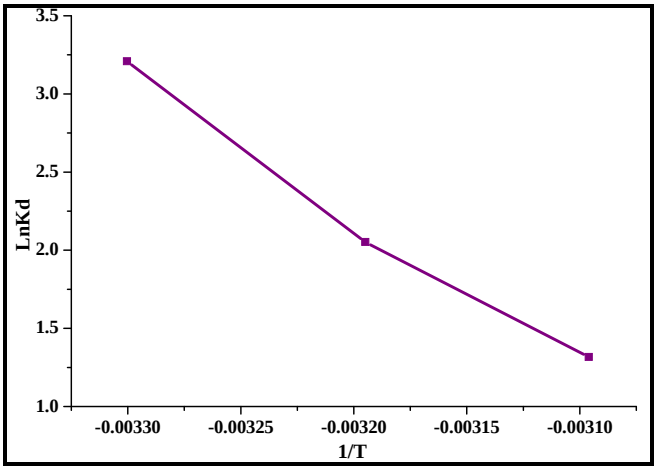

Figure 4.23 Thermodynamics plot for adsorption of Cr^{6+} on PANI

Table 4.6 Thermodynamics constants

T (K)	ΔG (kJ/mole)	ΔH (kJ/mole)	ΔS (J/moleK)
303	-7.9351	-77.124	-143.293
313	-5.6516		
323	-3.3682		
333	-1.0847		
343	1.1987		

4.5. Mechanism:

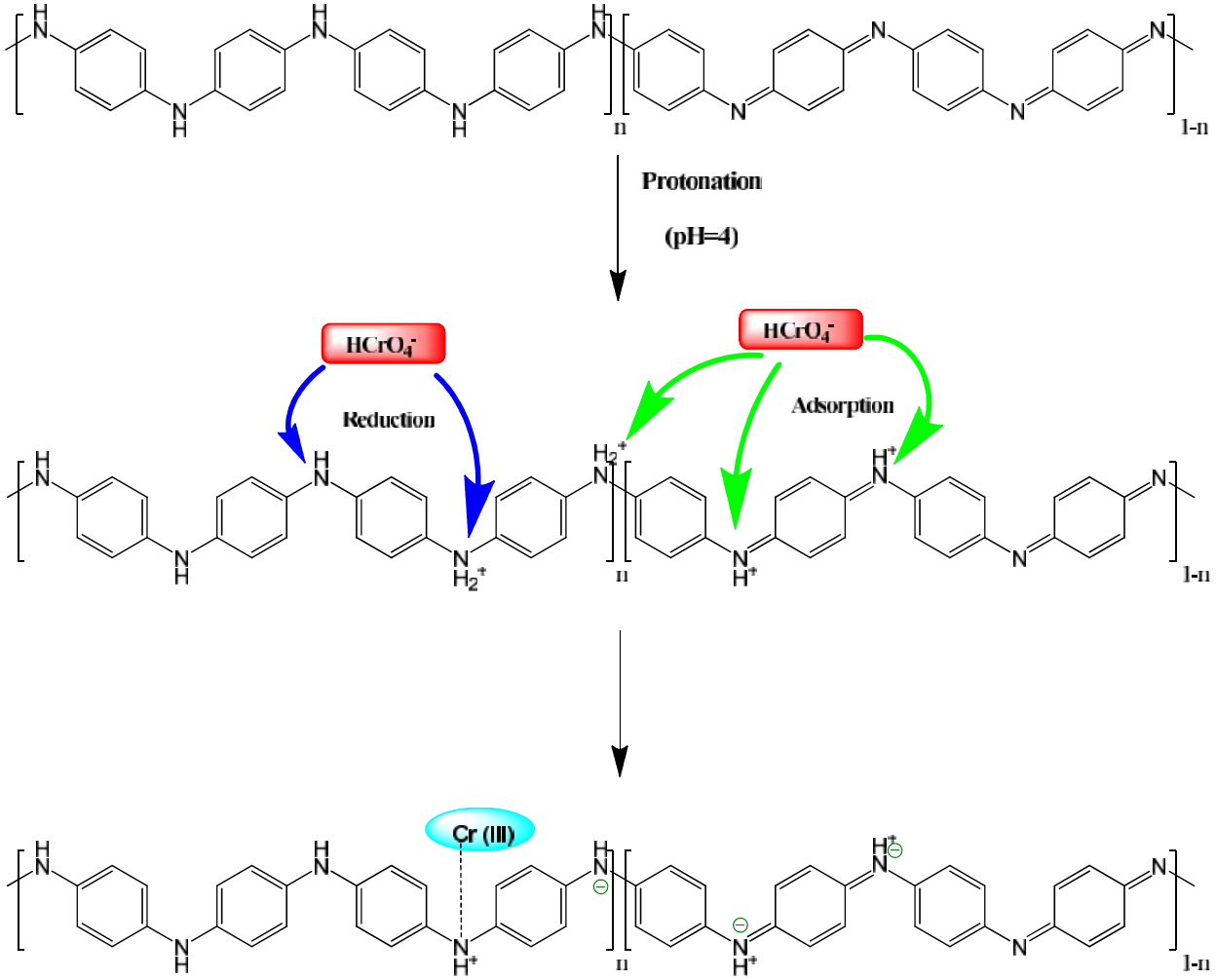

Scheme 1 Mechanism of chromium removal by PANI

The possible reaction between Cr^{6+} and synthesized PANI is shown in Scheme 1.

The proposed mechanism involved in the Cr^{6+} adsorption on the adsorbent can be understood as follows. Firstly, the surface of the adsorbent gets protonated and forms positively charged amine functional groups at lower pH. These protonated amine groups form surface complexes with the negatively charged Cr^{6+} ($HCrO_4^-$) through electrostatic attraction.

However Cr^{3+} was not getting leached into solution and it was observed that Cr^{6+} was getting completely reduced to Cr^{3+} and was present in reducing environment on PANI. With increasing contact time the percentage of Cr^{3+} in more reducing environment on polyaniline was increasing. No Cr^{6+} is detected on PANI by the XPS Cr2p spectra and diphenyl carbazide spectrophotometric method. The result suggests that all Cr^{6+} adsorbed on the surface of PANI has been totally reduced to Cr^{3+}. The peak of N1s spectra of Cr^{6+}-adsorbed PANI has been deconvoluted to two major components attributed to imine group (–N) and amine group (–NH–

), respectively.The Cr^{6+} is reduced to Cr^{3+} by the oxidation of benzenoid amine to quinoid imine indicated by FTIR , XPS and Raman signals corresponding to quinoid amine (Yu, Zhang, Wang, & Chai, 2013). The oxidation is evidenced by the presence of imine nitrogen in PANI-Cr as well as the reduction in amine nitrogen content in XPS spectra.

The protons are consumed during the reduction process of Cr^{6+}. Ion-exchange with protonated imine nitrogens in emeraldine salt facilitated the reduced Cr^{6+}(Cr^{3+}) to bind on PANI. The Cr^{3+} can also be further bound on the surface of PANI by chelation with imino groups (Harijan & Chandra, 2016; R. Zhang et al., 2010). An electron in sp^3 orbit of nitrogen atom of partially or fully oxidized forms of polyaniline makes a co-ordinate bond with positively charged Cr^{3+}. This is corroborated with total chromium ICP and XPS analysis

Comparing the observations of other researchers and our results it is felt that when mesoporous or nanostructured adsorbents are used and internal porous structure sites also play a role the mechanism of adsorption could be multilayered. The fitting of kinetic models and thermodynamics also then changes. It thus becomes important to study other multilayer models such as Halsey, Redlich Peterson a hybrid model before coming to a conclusion The PANI based adsorbents reported in literature have been compared in Table 7.2 of section 6 . However it is difficult to compare the adsorption efficiency of the adsorbents based on the arguments already made that different kinetic and isotherm model fits were obtained by various researchers and adsorption capacity was calculated at different pH.

4.6. Conclusion

Nano sized PANI was used for effective removal of Cr^{6+} from water. The removal of Cr^{6+} was governed by electrostatic interactions followed by reduction and was corroborated by Raman, FT-IR, ESR and XPS techniques. The Cr^{6+} adsorption governed by pseudo second order kinetics, was diffusion controlled and also involved multilayered adsorption process which was completed in 240 min. The adsorption data on PANI well fitted with Freundlich, Halsey and Elovich isotherm models. However it was not possible to regenerate PANI due to strong binding of Cr^{3+} with PANI. XRD studies indicated that PANI disintegrated to further nano sized samples after interacting with chromium.

References

Ansari, R. (2006). Application of Polyaniline and its Composites for Adsorption / Recovery of Chromium (VI) from Aqueous Solutions. *Composites*, (Vi), 88–94.

Ayad, M., & Zaghlol, S. (2012). Nanostructured crosslinked polyaniline with high surface area: Synthesis, characterization and adsorption for organic dye. *Chemical Engineering Journal*, *204–206*, 79–86. http://doi.org/http://dx.doi.org/10.1016/j.cej.2012.07.102

Baibarac, M., Mihut, L., Louarn, G., Mevellec, J. Y., Wery, J., Lefrant, S., & Baltog, I. (1999). Interfacial chemical effect evidenced on SERS spectra of polyaniline thin films deposited on rough metallic supports. *Journal of Raman Spectroscopy*, *30*(12), 1105–1113. http://doi.org/10.1002/(sici)1097-4555(199912)30:12<1105::aid-jrs507>3.3.co;2-v

Bhadra, S., Khastgir, D., Singha, N. K., & Lee, J. H. (2009). Progress in preparation, processing and applications of polyaniline. *Progress in Polymer Science (Oxford)*. http://doi.org/10.1016/j.progpolymsci.2009.04.003

Bhaumik, M., Maity, A., Srinivasu, V. V., & Onyango, M. S. (2012). Removal of hexavalent chromium from aqueous solution using polypyrrole-polyaniline nanofibers. *Chemical Engineering Journal*, *181–182*, 323–333. http://doi.org/10.1016/j.cej.2011.11.088

Cao, Y., Smith, P., & Heeger, A. J. (1992). Counter-ion induced processibility of conducting polyaniline and of conducting polyblends of polyaniline in bulk polymers. *Synthetic Metals*, *48*(1), 91–97. http://doi.org/10.1016/0379-6779(92)90053-L

Chakraborty, M., Mukherjee, D. C., & Mandal, B. M. (2000). Dispersion polymerization of aniline in different media: a UV-visible spectroscopic and kinetic study. *Langmuir*, *16*(6), 2482–2488. http://doi.org/10.1021/la990943d

Chávez-Guajardo, A. E., Medina-Llamas, J. C., Maqueira, L., Andrade, C. A. S., Alves, K. G. B., & de Melo, C. P. (2015). Efficient removal of Cr (VI) and Cu (II) ions from aqueous media by use of polypyrrole/maghemite and polyaniline/maghemite magnetic nanocomposites. *Chemical Engineering Journal*, *281*(Vi), 826–836. http://doi.org/10.1016/j.cej.2015.07.008

Chen, J., Hong, X., Xie, Q., Li, D., & Zhang, Q. (2014). Sepiolite Fiber Oriented-Polypyrrole Nano fi bers for E ffi cient Chromium (VI) Removal from Aqueous Solution, (Vi).

Chiou, N. R., & Epstein, A. J. (2005). Polyaniline nanofibers prepared by dilute polymerization. *Advanced Materials*. http://doi.org/10.1002/adma.200401000

Ciric -Marjanovic, Gordana Trchova, M., & Stejskal, J. (2008). The chemical oxidative polymerization of aniline in water: Raman spectroscopy. *Journal of Raman Spectroscopy*, *39*(April), 1375–1387. http://doi.org/10.1002/jrs

Collins, J. S., & Goldsmith, T. H. (1981). Spectral properties of fluorescence induced by glutaraldehyde fixation. *The Journal of Histochemistry and Cytochemistry*, *29*(3), 411–414. http://doi.org/10.1177/29.3.6787116

Colomban, P., Folch, S., & Gruger, A. (1999). Vibrational study of short-range order and structure of polyaniline bases and salts. *Macromolecules*, *32*(9), 3080–3092. http://doi.org/10.1021/ma981018l

Dhand, C., Singh, S. P., Arya, S. K., Datta, M., & Malhotra, B. D. (2007). Cholesterol biosensor based on electrophoretically deposited conducting polymer film derived from nano-structured polyaniline colloidal suspension. *Analytica Chimica Acta*, *602*(2), 244–251. http://doi.org/http://dx.doi.org/10.1016/j.aca.2007.09.028

Ding, Z., Sanchez, T., Labouriau, A., Iyer, S., Larson, T., Currier, R., … Yang, D. (2010). Characterization of reaction intermediate aggregates in aniline oxidative polymerization at low proton concentration. *Journal of Physical Chemistry B*, *114*(32), 10337–10346. http://doi.org/10.1021/jp102623z

Du, J., Zhang, J., Han, B., Liu, Z., & Wan, M. (2005). Polyaniline microtubes synthesized via supercritical CO2 and aqueous interfacial polymerization. *Synthetic Metals*, *155*(3), 523–526. http://doi.org/10.1016/j.synthmet.2005.07.336

Epstein, A. J., Ginder, J. ., Zuo, F., Bigelow, R. ., Woo, H.-S., Tanner, D. ., & A.F.Richter. (1987). Insulator-to-metal transition in polyaniline, *18*, 303–309.

Farhadi, K., Zebhi, H., Moghadam, P. N., Es'haghi, M., & Ashassi-Sorkhabi, H. (2014). Electrochemical preparation of nano-colloidal polyaniline in polyacid matrix and its application to the corrosion protection of 430SS. *Synthetic Metals*, *195*, 29–35. http://doi.org/http://dx.doi.org/10.1016/j.synthmet.2014.05.002

Farrell, S. T., & Breslin, C. B. (2004). Reduction of Cr(VI) at a polyaniline film: Influence of film thickness and oxidation state. *Environmental Science and Technology*, *38*(17), 4671–4676. http://doi.org/10.1021/es0498585

Fei, J., Cui, Y., Yan, X., Yang, Y., Wang, K., & Li, J. (2009). Controlled fabrication of polyaniline spherical and cubic shells with hierarchical nanostructures. *ACS Nano*, *3*(11), 3714–3718. http://doi.org/10.1021/nn900921v

Feng, X. M., Li, R. M., Ma, Y. W., Chen, R. F., Shi, N. E., Fan, Q. L., & Huang, W. (2011). One-step electrochemical synthesis of graphene/polyaniline composite film and its applications. *Advanced Functional Materials*, *21*(15), 2989–2996. http://doi.org/10.1002/adfm.201100038

Fernandez, R. O., & Pizarro, R. a. (1997). High-performance liquid chromatographic analysis of

Pseudomonas aeruginosa phenazines. *Journal of Chromatography A*, *771*, 99–104. http://doi.org/10.1016/S0021-9673(97)00092-7

Folch, S., Gruger, A., Régis, A., & Colomban, P. (1996). Optical and vibrational spectra of sols/solutions of polyaniline: Water as secondary dopant. *Synthetic Metals*, *81*(2–3), 221–225. http://doi.org/10.1016/S0379-6779(96)03745-9

Galasso, V. (2008). A DFT characterization of the structures and UV/vis absorption spectra of mauveine dyes. *Chemical Physics Letters*, *457*(1–3), 250–253. http://doi.org/10.1016/j.cplett.2008.03.072

Gao, Y., Chen, C., Tan, X., Xu, H., & Zhu, K. (2016). Polyaniline-modified 3D-flower-like molybdenum disulfide composite for efficient adsorption/photocatalytic reduction of Cr(VI). *Journal of Colloid and Interface Science*, *476*, 62–70. http://doi.org/http://dx.doi.org/10.1016/j.jcis.2016.05.022

Germain, J., Fréchet, J. M. J., & Svec, F. (2007). Hypercrosslinked polyanilines with nanoporous structure and high surface area: potential adsorbents for hydrogen storage. *Journal of Materials Chemistry*, *17*(47), 4989–4997. http://doi.org/10.1039/b711509a

Golczak, S., Kanciurzewska, A., Fahlman, M., Langer, K., & Langer, J. J. (2008). Comparative XPS surface study of polyaniline thin films. *Solid State Ionics*, *179*(39), 2234–2239. http://doi.org/10.1016/j.ssi.2008.08.004

Gu, H., Guo, J., Zhang, X., He, Q., Huang, Y., Colorado, H. A., … Guo, Z. (2013). Giant magnetoresistive phosphoric acid doped polyaniline-silica nanocomposites. *Journal of Physical Chemistry C*, *117*(12), 6426–6436. http://doi.org/10.1021/jp311471f

Gu, H., Rapole, S. B., Sharma, J., Huang, Y., Cao, D., Colorado, H. A., … Guo, Z. (2012). Magnetic polyaniline nanocomposites toward toxic hexavalent chromium removal. *RSC Advances*, *2*(29), 11007–11018. http://doi.org/10.1039/c2ra21991c

Gu, H., Tadakamalla, S., Zhang, X., Huang, Y., Jiang, Y., Colorado, H. A., … Guo, Z. (2013). Epoxy resin nanosuspensions and reinforced nanocomposites from polyaniline stabilized multi-walled carbon nanotubes. *J. Mater. Chem. C*, *1*(4), 729–743. http://doi.org/10.1039/C2TC00379A

Gu, H., Wei, H., Guo, J., Haldolaarachige, N., Young, D. P., Wei, S., & Guo, Z. (2013). Hexavalent chromium synthesized polyaniline nanostructures: Magnetoresistance and electrochemical energy storage behaviors. *Polymer (United Kingdom)*, *54*(21), 5974–5985. http://doi.org/10.1016/j.polymer.2013.08.020

Guo, X., Fei, G. T., Su, H., & Zhang, L. De. (2011). High-Performance and Reproducible Polyaniline Nanowire / Tubes for Removal of Cr (VI) in Aqueous Solution. *The Journal of*

Physical Chemistry C, *115*(Vi), 1608–1613.

Harijan, D. K. L., & Chandra, V. (2016). Polyaniline functionalized graphene sheets for treatment of toxic hexavalent chromium. *Journal of Environmental Chemical Engineering*, *4*(3), 3006–3012. http://doi.org/10.1016/j.jece.2016.06.014

Hena, S. (2010). Removal of chromium hexavalent ion from aqueous solutions using biopolymer chitosan coated with poly 3-methyl thiophene polymer. *Journal of Hazardous Materials*, *181*(1–3), 474–479. http://doi.org/10.1016/j.jhazmat.2010.05.037

Hong, Y., Hwang, S., Yoon, D. S., & Yang, J. (2015). Scattering analysis of single polyaniline nanoparticles for acidic environmental sensing. *Sensors and Actuators B: Chemical*, *218*, 31–36. http://doi.org/http://dx.doi.org/10.1016/j.snb.2015.04.098

Huang, J., & Kaner, R. B. (2006). The intrinsic nanofibrillar morphology of polyaniline. *Chemical Communications*, (4), 367–76. http://doi.org/10.1039/b510956f

Ithurbide, A., Frateur, I., Galtayries, A., & Marcus, P. (2007). XPS and flow-cell EQCM study of albumin adsorption on passivated chromium surfaces: Influence of potential and pH. *Electrochimica Acta*, *53*(3 SPEC. ISS.), 1337–1346. http://doi.org/10.1016/j.electacta.2007.04.109

Izumi, C. M. S., Andrade, G. F. S., & Temperini, M. L. a. (2008). Surface-enhanced resonance Raman scattering of polyaniline on silver and gold colloids. *The Journal of Physical Chemistry. B*, *112*(51), 16334–40. http://doi.org/10.1021/jp805373s

Jain, M., & Annapoorni, S. (2010). Raman study of polyaniline nanofibers prepared by interfacial polymerization. *Synthetic Metals*, *160*(15–16), 1727–1732. http://doi.org/10.1016/j.synthmet.2010.06.008

Jin, Z., Su, Y., & Duan, Y. (2001). A novel method for polyaniline synthesis with the immobilized horseradish peroxidase enzyme. *Synthetic Metals*, *122*(2), 237–242. http://doi.org/10.1016/S0379-6779(00)00287-3

Karim, M. R., Lee, C. J., Park, Y. T., & Lee, M. S. (2005). SWNTs coated by conducting polyaniline: Synthesis and modified properties. *Synthetic Metals*, *151*(2), 131–135. http://doi.org/10.1016/j.synthmet.2005.03.012

Karthik, R., & Meenakshi, S. (2014a). Facile synthesis of cross linked-chitosan-grafted-polyaniline composite and its Cr(VI) uptake studies. *International Journal of Biological Macromolecules*, *67*, 210–219. http://doi.org/10.1016/j.ijbiomac.2014.03.035

Karthik, R., & Meenakshi, S. (2014b). Removal of hexavalent chromium ions using polyaniline/silica gel composite. *Journal of Water Process Engineering*, *1*, 37–45. http://doi.org/10.1016/j.jwpe.2014.03.001

Karthik, R., & Meenakshi, S. (2015a). Removal of Cr(VI) ions by adsorption onto sodium alginate-polyaniline nanofibers. *International Journal of Biological Macromolecules*, *72*, 711–717. http://doi.org/10.1016/j.ijbiomac.2014.09.023

Karthik, R., & Meenakshi, S. (2015b). Synthesis, characterization and Cr(VI) uptake study of polyaniline coated chitin. *International Journal of Biological Macromolecules*, *72*, 235–242. http://doi.org/10.1016/j.ijbiomac.2014.08.022

Kim, M. K., Shanmuga Sundaram, K., Anantha Iyengar, G., & Lee, K. P. (2015). A novel chitosan functional gel included with multiwall carbon nanotube and substituted polyaniline as adsorbent for efficient removal of chromium ion. *Chemical Engineering Journal*, *267*, 51–64. http://doi.org/10.1016/j.cej.2014.12.091

Kousalya, G. N., Rajiv Gandhi, M., & Meenakshi, S. (2010). Sorption of chromium (VI) using modified forms of chitosan beads. *International Journal of Biological Macromolecules*, *47*(2), 308–15. http://doi.org/10.1016/j.ijbiomac.2010.03.010

Krinichnyi, V. I., Roth, H. K., Schrodner, M., & Wessling, B. (2006). EPR study of polyaniline highly doped by p-toluenesulfonic acid. *Polymer*, *47*(21), 7460–7468. http://doi.org/10.1016/j.polymer.2006.08.025

Krishnani, K. K., Srinives, S., Mohapatra, B. C., Boddu, V. M., Hao, J., Meng, X., & Mulchandani, A. (2013). Hexavalent chromium removal mechanism using conducting polymers. *Journal of Hazardous Materials*, *252–253*, 99–106. http://doi.org/10.1016/j.jhazmat.2013.01.079

Kumar, P. A., & Chakraborty, S. (2009). Fixed-bed column study for hexavalent chromium removal and recovery by short-chain polyaniline synthesized on jute fiber. *Journal of Hazardous Materials*, *162*(2–3), 1086–1098. http://doi.org/10.1016/j.jhazmat.2008.05.147

Kumar, P. A., Chakraborty, S., & Ray, M. (2008). Removal and recovery of chromium from wastewater using short chain polyaniline synthesized on jute fiber. *Chemical Engineering Journal*, *141*(1–3), 130–140. http://doi.org/10.1016/j.cej.2007.11.004

Kumar, R., Ansari, M. O., & Barakat, M. A. (2013). DBSA doped polyaniline/multi-walled carbon nanotubes composite for high efficiency removal of Cr(VI) from aqueous solution. *Chemical Engineering Journal*, *228*, 748–755. http://doi.org/10.1016/j.cej.2013.05.024

Lei, Y., Qian, X., Shen, J., & An, X. (2012). Integrated reductive/adsorptive detoxification of Cr(VI)-contaminated water by polypyrrole/cellulose fiber composite. *Industrial and Engineering Chemistry Research*, *51*(31), 10408–10415. http://doi.org/10.1021/ie301136g

lekha, P. C., Subramanian, S., Yi, J., Dhanuskodi, S., & Padiyan, D. P. (2010). Intercalation of polyoxomolybdate in polyaniline matrix: Enhancement in {AC} impedance and gas sensing

properties. *Materials Chemistry and Physics*, *122*(2–3), 431–438. http://doi.org/http://dx.doi.org/10.1016/j.matchemphys.2010.03.019

Ležaić, A. J., Bajuk-Bogdanović, D., Radoičić, M., Mirsky, V. M., & Ciric-Marjanovic, G. (2016). Influence of synthetic conditions on the structure and electrical properties of nanofibrous polyanilines and their nanofibrous carbonized forms. *Synthetic Metals*, *214*, 35–44. http://doi.org/10.1016/j.synthmet.2016.01.015

Li, G., Jiang, L., & Peng, H. (2007). One-dimensional polyaniline nanostructures with controllable surfaces and diameters using vanadic acid as the oxidant. *Macromolecules*, *40*(22), 7890–7894. http://doi.org/10.1021/ma070650o

Li, G., Li, Y., Li, Y., Peng, H., & Chen, K. (2011). Polyaniline nanorings and flat hollow capsules synthesized by in situ sacrificial oxidative templates. *Macromolecules*, *44*(23), 9319–9323. http://doi.org/10.1021/ma2014854

Li, N., Yang, S., Chen, J., Gao, J., He, H., & Sun, C. (2016). Electro-adsorption of tetracycline from aqueous solution by carbonized pomelo peel and composite with aniline. *Applied Surface Science*, *386*, 460–466. http://doi.org/http://dx.doi.org/10.1016/j.apsusc.2016.05.173

Li, Q., Sun, L., Zhang, Y., Qian, Y., & Zhai, J. (2011). Characteristics of equilibrium, kinetics studies for adsorption of Hg(II) and Cr(VI) by polyaniline/humic acid composite. *Desalination*, *266*(1–3), 188–194. http://doi.org/10.1016/j.desal.2010.08.025

Li, R., Liu, L., & Yang, F. (2014). Removal of aqueous Hg (II) and Cr (VI) using phytic acid doped polyaniline / cellulose acetate composite membrane. *Journal of Hazardous Materials*, *280*, 20–30. http://doi.org/10.1016/j.jhazmat.2014.07.052

Liu, X., Zhou, W., Qian, X., Shen, J., & An, X. (2013). Polyaniline/cellulose fiber composite prepared using persulfate as oxidant for Cr(VI)-detoxification. *Carbohydrate Polymers*, *92*(1), 659–661. http://doi.org/10.1016/j.carbpol.2012.09.083

Luo, C., Peng, H., Zhang, L., Lu, G. L., Wang, Y., & Travas-Sejdic, J. (2011). Formation of nano-/microstructures of polyaniline and its derivatives. *Macromolecules*, *44*(17), 6899–6907. http://doi.org/10.1021/ma201350m

MacDiarmid, A. G., Manohar, S. K., Masters, J. G., Sun, Y., Weiss, H., & Epstein, A. J. (1991). Polyaniline: Synthesis and properties of pernigraniline base. *Synthetic Metals*, *41*(1–2), 621–626. http://doi.org/10.1016/0379-6779(91)91145-Z

Murphy, V., Tofail, S. A. M., Hughes, H., & McLoughlin, P. (2009). A novel study of hexavalent chromium detoxification by selected seaweed species using SEM-EDX and XPS analysis. *Chemical Engineering Journal*, *148*(2–3), 425–433.

http://doi.org/10.1016/j.cej.2008.09.029

Najim, T. S., & Salim, A. J. (2014). Polyaniline nanofibers and nanocomposites: Preparation, characterization, and application for Cr(VI) and phosphate ions removal from aqueous solution. *Arabian Journal of Chemistry*. http://doi.org/10.1016/j.arabjc.2014.02.008

Ogoshi, T., Hasegawa, Y., Aoki, T., Ishimori, Y., Inagi, S., & Yamagishi, T. A. (2011). Reduction of emeraldine base form of polyaniline by pillar[5]arene based on formation of poly(pseudorotaxane) structure. *Macromolecules*, *44*(19), 7639–7644. http://doi.org/10.1021/ma2016979

Okamoto, H., Okamoto, M., & Kotaka, T. (1998). Structure development in polyaniline films during electrochemical polymerization. II: Structure and properties of polyaniline films prepared via electrochemical polymerization. *Polymer*, *39*(18), 4359–4367. Retrieved from http://www.scopus.com/scopus/inward/record.url?eid=2-s2.0-0032136170&partnerID=40

Olad, A., & Nabavi, R. (2007). Application of polyaniline for the reduction of toxic Cr(VI) in water. *Journal of Hazardous Materials*, *147*(3), 845–851. http://doi.org/10.1016/j.jhazmat.2007.01.083

Pan, L., Pu, L., Shi, Y., Song, S., Xu, Z., Zhang, R., & Zheng, Y. (2007). Synthesis of polyaniline nanotubes with a reactive template of manganese oxide. *Advanced Materials*, *19*(3), 461–464. http://doi.org/10.1002/adma.200602073

Pan, L., Pu, L., Shi, Y., Sun, T., Zhang, R., & Zheng, Y. (2006). Hydrothermal synthesis of polyaniline mesostructures. *Advanced Functional Materials*, *16*(10), 1279–1288. http://doi.org/10.1002/adfm.200500543

Park, D., Yun, Y. S., & Park, J. M. (2008). XAS and XPS studies on chromium-binding groups of biomaterial during Cr(VI) biosorption. *Journal of Colloid and Interface Science*, *317*(1), 54–61. http://doi.org/10.1016/j.jcis.2007.09.049

Pei, Z., Ding, L., Lu, M., Fan, Z., Weng, S., Hu, J., & Liu, P. (2014). Synergistic Effect in Polyaniline-Hybrid Defective ZnO with Enhanced Photocatalytic Activity and Stability. *The Journal of Physical Chemistry C*, *118*, 9570–9577.

Pereira Da Silva, J. E., De Faria, D. L. A., Cordoba De Torresi, S. I., & Temperini, M. L. A. (2000). Influence of thermal treatment on doped polyaniline studied by resonance Raman spectroscopy. *Macromolecules*, *33*(8), 3077–3083. http://doi.org/10.1021/ma990801q

Qaiser, A. A., Hyland, M. M., & Patterson, D. A. (2012). Effects of various polymerization techniques on {PANI} deposition at the surface of cellulose ester microporous membranes: {XPS} and electrical conductivity studies. *Synthetic Metals*, *162*(11–12), 958–967. http://doi.org/http://dx.doi.org/10.1016/j.synthmet.2012.04.009

Qiu, B., Xu, C., Sun, D., Wang, Q., Gu, H., Zhang, X., … Wei, S. (2015). Polyaniline coating with various substrates for hexavalent chromium removal. *Applied Surface Science*, *334*, 7–14. http://doi.org/10.1016/j.apsusc.2014.07.039

Qiu, B., Xu, C., Sun, D., Wei, H., Zhang, X., Guo, J., & Wang, Q. (2014). Polyaniline coating on carbon fiber fabrics for improved hexavalent chromium removal. *RSC Advances*, *4*, 29855–29865. http://doi.org/10.1039/c4ra01700e

Qiu, B., Xu, C., Sun, D., Yi, H., Guo, J., Zhang, X., … Wei, S. (2014). Polyaniline coated ethyl cellulose with improved hexavalent chromium removal. *ACS Sustainable Chemistry and Engineering*, *2*(8), 2070–2080. http://doi.org/10.1021/sc5003209

Ram, M. K., Mascetti, G., Paddeu, S., Maccioni, E., & Nicolini, C. (1997). Optical, structural and fluorescence microscopic studies on reduced form of polyaniline: the leucoemeraldine base. *Synthetic Metals*, *89*(1), 63–69. http://doi.org/10.1016/S0379-6779(97)81194-0

Ruotolo, L. A. M., & Gubulin, J. C. (2005). Chromium(VI) reduction using conducting polymer films. *Reactive and Functional Polymers*, *62*(2), 141–151. http://doi.org/10.1016/j.reactfunctpolym.2004.11.004

Ruotolo, L. A. M., Santos-Júnior, D. S., & Gubulin, J. C. (2006). Electrochemical treatment of effluents containing Cr(VI). Influence of pH and current on the kinetic. *Water Research*, *40*(8), 1555–1560. http://doi.org/10.1016/j.watres.2006.02.005

Samani, M. R., Borghei, S. M., Olad, A., & Chaichi, M. J. (2010). Removal of chromium from aqueous solution using polyaniline - Poly ethylene glycol composite. *Journal of Hazardous Materials*, *184*(1–3), 248–254. http://doi.org/10.1016/j.jhazmat.2010.08.029

Shimano, J. Y., & MacDiarmid, A. G. (2001). Polyaniline, a dynamic block copolymer: Key to attaining its intrinsic conductivity? *Synthetic Metals*, *123*(2), 251–262. http://doi.org/10.1016/S0379-6779(01)00293-4

Sonmez, G., Sonmez, H. B., Shen, C. K. F., & Wudl, F. (2004). Red, green, and blue colors in polymeric electrochromics. *Advanced Materials*, *16*(21), 1905–1908. http://doi.org/10.1002/adma.200400546

Srinivas, C., Srinivasu, D., Kavitha, B., Narsimlu, N., & Siva Kumar 5, K. (2012). Synthesis and Characterization of Nano Size Conducting Polyaniline. *IOSR Journal of Applied Physics*, *1*(5), 12–15. Retrieved from www.iosrjournals.org

Stejskal, J., & Gilbert, R. G. (2002). Polyaniline. Preparation of a conducting polymer. *Pure and Applied Chemistry*, *74*(5), 857–867. http://doi.org/10.1351/pac200274050857

Stejskal, J., Sapurina, I., & Trchova, M. (2010). Polyaniline nanostructures and the role of aniline oligomers in their formation. *Progress in Polymer Science (Oxford)*, *35*(12), 1420–

1481. http://doi.org/10.1016/j.progpolymsci.2010.07.006

Tang, L., Fang, Y., Pang, Y., Zeng, G., Wang, J., Zhou, Y., … Chen, J. (2014). Synergistic adsorption and reduction of hexavalent chromium using highly uniform polyaniline-magnetic mesoporous silica composite. *Chemical Engineering Journal*, *254*, 302–312. http://doi.org/10.1016/j.cej.2014.05.119

Tian, Y., Li, H., Liu, Y., Cui, G., Sun, Z., & Yan, S. (2016). Morphology-dependent enhancement of template-guided tunable polyaniline nanostructures for the removal of Cr(VI). *RSC Adv.*, *6*(13), 10478–10486. http://doi.org/10.1039/C5RA25630E

Trchova, M., Moravkova, Z., Blaha, M., & Stejskal, J. (2014). Raman spectroscopy of polyaniline and oligoaniline thin films. *Electrochimica Acta*, *122*, 28–38. http://doi.org/10.1016/j.electacta.2013.10.133

Trchova, M., Moravkova, Z., Dybal, J., & Stejskal, J. (2014). Detection of aniline oligomers on polyaniline-gold interface using resonance Raman scattering. *ACS Applied Materials and Interfaces*, *6*(2), 942–950. http://doi.org/10.1021/am404252f

Trchova, M., Sedenkova, I., Konyushenko, E. N., Stejskal, J., & Ciric-Marjanovic, G. (2006). Evolution of polyaniline nanotubes: The oxidation of aniline in water. *Journal of Physical Chemistry B*, *110*(19), 9461–9468. http://doi.org/10.1021/jp057528g

Tsukerblat, B. S., Kuyavskaya, B. Y., Fainzilberg, V. E., & Belinskii, M. I. (1984). ESR spectra of trimeric heteronuclear clusters. II. Paramagnetic resonance of heteronuclear chromium and iron carboxylates. *Chemical Physics*, *90*(3), 373–386. http://doi.org/http://dx.doi.org/10.1016/0301-0104(84)85333-1

Wang, J., Pan, K., He, Q., & Cao, B. (2013). Polyacrylonitrile/polypyrrole core/shell nanofiber mat for the removal of hexavalent chromium from aqueous solution. *Journal of Hazardous Materials*, *244–245*, 121–129. http://doi.org/10.1016/j.jhazmat.2012.11.020

Wang, J. S., Peng, R. T., Yang, J. H., Liu, Y. C., & Hu, X. J. (2011). Preparation of ethylenediamine-modified magnetic chitosan complex for adsorption of uranyl ions. *Carbohydrate Polymers*, *84*(3), 1169–1175. http://doi.org/10.1016/j.carbpol.2011.01.007

Wang, J., Zhang, K., & Zhao, L. (2014). Sono-assisted synthesis of nanostructured polyaniline for adsorption of aqueous Cr(VI): Effect of protonic acids. *Chemical Engineering Journal*, *239*, 123–131. http://doi.org/10.1016/j.cej.2013.11.006

Wang, K., Huang, J., & Wei, Z. (2010). Conducting Polyaniline Nanowire Arrays for High Performance Supercapacitors. *The Journal of Physical Chemistry C*, *114*(17), 8062–8067. http://doi.org/10.1021/jp9113255

Watanabe, A., Mori, K., Iwasaki, Y., Nakamura, Y., & Niizuma, S. (1987). Electrochromism of

Polyaniline Film Prepared by Electrochemical Polymerization. *Macromolecules*, *20*, 1793–1796. http://doi.org/10.1021/ma00174a015

Wen, T., Fan, Q., Tan, X., Chen, Y., Chen, C., Xu, A., & Wang, X. (2016). A core–shell structure of polyaniline coated protonic titanate nanobelt composites for both Cr(<scp>vi</scp>) and humic acid removal. *Polym. Chem.*, *7*(4), 785–794. http://doi.org/10.1039/C5PY01721A

Xia, X., Hao, Q., Lei, W., Wang, W., Sun, D., & Wang, X. (2012). Nanostructured ternary composites of graphene/Fe2O3/polyaniline for high-performance supercapacitors. *Journal of Materials Chemistry*, *22*(33), 16844. http://doi.org/10.1039/c2jm33064d

Yang, G., Tang, L., Cai, Y., Zeng, G., Guo, P., Chen, G., … Xiong, W. (2014). RSC Advances Effective removal of Cr (VI) through adsorption and reduction by magnetic mesoporous carbon incorporated with polyaniline. *RSC Advances*, *4*, 58362–58371. http://doi.org/10.1039/C4RA08432B

Yavuz, A. G., Dincturk-Atalay, E., Uygun, A., Gode, F., & Aslan, E. (2011). A comparison study of adsorption of Cr(VI) from aqueous solutions onto alkyl-substituted polyaniline/chitosan composites. *Desalination*, *279*(1–3), 325–331. http://doi.org/10.1016/j.desal.2011.06.034

Yu, W., Zhang, L., Wang, H., & Chai, L. (2013). Adsorption of Cr(VI) using synthetic poly(m-phenylenediamine). *Journal of Hazardous Materials*, *260*, 789–795. http://doi.org/10.1016/j.jhazmat.2013.06.045

Yue, J., & Epstein, a J. (1991). Xps Study of Self-Doped Conducting Polyaniline and Parent Systems. *Macromolecules*, *24*(15), 4441–4445. http://doi.org/Doi 10.1021/Ma00015a030

Zhang, R., Ma, H., & Wang, B. (2010). Removal of chromium(VI) from aqueous solutions using polyaniline doped with sulfuric acid. *Industrial and Engineering Chemistry Research*, *49*(20), 9998–10004. http://doi.org/10.1021/ie1008794

Zhang, S., Zeng, M., Xu, W., Li, J., Li, J., Xu, J., & Wang, X. (2013). Polyaniline nanorods dotted on graphene oxide nanosheets as a novel super adsorbent for Cr(VI). *Dalton Transactions (Cambridge, England : 2003)*, *42*, 7854–8. http://doi.org/10.1039/c3dt50149c

Zhang, X., Chechik, V., Smith, D. K., Walton, P. H., & Duhme-Klair, A. K. (2008). Controlled synthesis of optically active polyaniline nanorods and nanostructured gold microspheres using tetrachloroaurate as an efficient oxidant of aniline. *Macromolecules*, *41*(10), 3417–3421. http://doi.org/10.1021/ma800134w

Zhang, Z., Wei, Z., & Wan, M. (2002). Nanostructures of polyaniline doped with inorganic acids. *Macromolecules*, *35*(15), 5937–5942. http://doi.org/10.1021/ma020199v

Zhao, Y., Zhang, Z., Yu, L., & Tang, Q. (2016). Electrospinning of polyaniline microfibers for anticorrosion coatings: An avenue of enhancing anticorrosion behaviors. *Synthetic Metals*, *212*, 84–90. http://doi.org/http://dx.doi.org/10.1016/j.synthmet.2015.12.007

Zheng, Y., Wang, W., Huang, D., & Wang, A. (2012). Kapok fiber oriented-polyaniline nanofibers for efficient Cr(VI) removal. *Chemical Engineering Journal*, *191*, 154–161. http://doi.org/10.1016/j.cej.2012.02.088

Zhu, K., Gao, Y., Tan, X., & Chen, C. (2016). Polyaniline-Modified Mg/Al Layered Double Hydroxide Composites and Their Application in Efficient Removal of Cr(VI). *ACS Sustainable Chemistry & Engineering*, (Vi), acssuschemeng.6b00922. http://doi.org/10.1021/acssuschemeng.6b00922

Zuo, X., & Balasubramanian, R. (2013). Evaluation of a novel chitosan polymer-based adsorbent for the removal of chromium (III) in aqueous solutions. *Carbohydrate Polymers*, *92*(2), 2181–2186. http://doi.org/10.1016/j.carbpol.2012.12.009